

1 Long-term trends in pH in Japanese coastal seawater

2
3 Miho Ishizu¹, Yasumasa Miyazawa¹, Tomohiko Tsunoda², Tsuneo Ono³

4
5 ¹E-mail: mishizu@jamstec.go.jp

6 ¹E-mail: miyazawa@jamstec.go.jp

7 Japan Agency for Marine-Earth Science and Technology, Environmental Variability Prediction and
8 Application Research Group, Yokohama Institute for Earth Sciences, 3173-25 Showa-machi,
9 Kanagawa-ku, Yokohama 236-0001, Japan

10 Tel: +81-45-778-5875

11 Fax: +81-45-778-5497

12

13 ²E-mail: t-tsunoda@spf.or.jp

14 The Ocean Policy Research Institute of the Sasakawa Peace Foundation, 1-15-16, Toranomom Minato-
15 ku, Tokyo 105-8524, Japan

16

17 ³E-mail: tono@affrc.go.jp

18 Japan Fisheries Research Education Agency, 15F Queen's Tower B, 2-3-3 Minato Mirai, Nishi-ku,
19 Yokohama, Kanagawa 220-6115, Japan

20

21 **Abstract**

22 In recent decades, acidification of the open ocean has shown consistent increases. However,
23 analysis of long-term data in coastal seawater shows that the pH is highly variable because of coastal

24 processes and anthropogenic carbon inputs. It is therefore important to understand how anthropogenic
25 carbon inputs and other natural or anthropogenic factors influence the temporal trends in pH in coastal
26 seawater. Using water quality data collected at 289 monitoring sites as part of the Water Pollution
27 Control Program, we evaluated the long-term trends in the $\text{pH}_{\text{insitu}}$ in Japanese coastal seawater at
28 ambient temperature from 1978 to 2009. We found that the annual maximum $\text{pH}_{\text{insitu}}$, which generally
29 represents the pH of surface waters in winter, had decreased at 75% of the sites, but had increased at
30 the remaining sites. The temporal trend in the annual minimum $\text{pH}_{\text{insitu}}$, which generally represents the
31 pH of subsurface water in summer, also showed a similar distribution, although it was relatively
32 difficult to interpret the trends of annual minimum $\text{pH}_{\text{insitu}}$ because the sampling depths differed from
33 station to station. The annual maximum $\text{pH}_{\text{insitu}}$ decreased at an average rate of -0.0024 yr^{-1} , with
34 relatively large deviations from the average value. Detailed analysis suggested that the decrease in pH
35 was caused partly by warming of winter surface waters in Japanese coastal seawater. The pH
36 normalized to 25°C , however, showed decreasing trends, suggesting that dissolved inorganic carbon
37 from anthropogenic sources was increasing in Japanese coastal seawater.

38

39 Keywords: pH, CO_2 , Global warming, Ocean acidification, Coastal
40 acidification/basification, Data analysis

41

42 1. Introduction

43 The effect of ocean acidification on several marine organisms, including calcifiers, is widely
44 acknowledged and is the topic of various marine research projects worldwide. Chemical variables
45 related to carbonate cycles are monitored in several ongoing ocean projects to determine whether the
46 rate of ocean acidification can be identified from changes in pH and other variables in the open ocean
47 (Gonzalez-Davila et al. 2007; Dore et al. 2009; Bates 2007; Bates et al. 2014; Midorikawa et al. 2010;
48 Olafsson et al. 2009; Wakita et al. 2017). Analysis of pH data measured in situ at the European Station
49 in the Canary Islands (ESTOC) in the North Atlantic from 1995 to 2003 and normalized to 25 °C
50 showed that the pH_{25} decreased at a rate of $0.0017 \pm 0.0005 \text{ yr}^{-1}$ (Gonzalez-Davila et al. 2007). Similarly,
51 analysis of the Hawaii Ocean Time series (HOT) (Dore et al. 2009) and the Bermuda Atlantic Time
52 Series (BATS) (Bates 2007) showed that the pH at ambient (in situ) sea surface temperature ($\text{pH}_{\text{insitu}}$)
53 decreased by 0.0019 ± 0.0002 and $0.0017 \pm 0.0001 \text{ yr}^{-1}$ from 1988 to 2007 and from 1983 to 2005,
54 respectively. Analysis of data collected along the hydrographic observation line at 137°E in the western
55 North Pacific by the Japanese Meteorological Agency (JMA) showed that the pH_{25} decreased by
56 $0.0013 \pm 0.0005 \text{ yr}^{-1}$ in summer and $0.0018 \pm 0.0002 \text{ yr}^{-1}$ in winter from 1983 to 2007 (Midorikawa et
57 al. 2010). The winter $\text{pH}_{\text{insitu}}$ in surface water in the Nordic Seas decreased at a rate of 0.0024 ± 0.0002
58 yr^{-1} from 1985 to 2008 (Olafsson et al. 2009). This rate was somewhat more rapid than the average
59 annual rates calculated for the other subtropical time series in the Atlantic Ocean, BATS, and ESTOC,
60 and was attributed to the air–sea CO_2 flux and buffering capacity (higher Revell factor) (Olafsson et
61 al. 2009), which were higher and lower than those in subtropical regions, respectively. Wakita et al.

62 (2017) estimated that the annual and winter $\text{pH}_{\text{insitu}}$ at station K2 in the subarctic western North Pacific
63 decreased at rates of 0.0025 and 0.0008 yr^{-1} , respectively, from 1999 to 2015. The lower rate in winter
64 was explained by increases in dissolved inorganic carbon (DIC) and total alkalinity (Alk) that resulted
65 from climate-related variations in ocean currents.

66 These long-term time series from various sites in the open ocean indicate consistent changes in
67 surface ocean carbon chemistry, which mainly reflect the uptake of anthropogenic CO_2 , with
68 consequences for ocean acidity. Coastal seawater, however, differ from the open ocean as they are
69 subjected to multiple influences, such as hydrological processes, land use in watersheds, nutrient inputs
70 (Duarte et al. 2013), changes in the structure of ecosystems caused by eutrophication (Borges and
71 Gypens 2010; Cai et al. 2011), marine pollution (Zeng et al. 2015), and variations in salinity (Sunda
72 and Cai 2012).

73 Duarte et al. (2013) hypothesized that anthropogenic pressures would cause the $\text{pH}_{\text{insitu}}$ of coastal
74 seawater to decrease (acidification) or increase (basification), depending on the balance between the
75 atmospheric CO_2 inputs and watershed exports of alkaline compounds, organic matter, and nutrients.
76 For example, in Chesapeake Bay, the $\text{pH}_{\text{insitu}}$ has shown temporal variations over the last 60 years,
77 presumably because of the combined influence of increases and decreases in $\text{pH}_{\text{insitu}}$ in the mesohaline
78 and polyhaline regions of the main part of the bay, respectively (Waldbusser et al., 2011; Duarte et al.,
79 2013).

80 These processes that occur only in coastal regions might cause increases or decreases in the rate of

81 acidification, meaning that the outcomes for coastal ecosystems in different regions will vary. At
82 present we have limited information about long-term changes in pH in coastal seawater, mainly
83 because of the difficulty involved in collecting continuous long-term data from coastal seawater around
84 an entire country at a spatial resolution that sufficiently covers the high regional variability in coastal
85 pH.

86 The Water Pollution Control Law (WPCL) was established in 1970 to deal with the serious
87 pollution of the Japanese aquatic environment in the 1950s and 1960s. Several environmental variables,
88 including $\text{pH}_{\text{insitu}}$, have been continuously measured in coastal waters since 1978, using consistent
89 methods enacted in the monitoring program under the leadership of the government, to help protect
90 coastal water and groundwater from pollution and retain the integrity of water environments. The errors
91 in pH measurements collected in this program were assessed as outlined in the JIS Z8802 (JIS;
92 Japanese Industrial Standard) standard protocol (2011) that corresponds to the ISO 10523 (ISO;
93 International Organization for Standardization) standard protocol. Compared with the specialized
94 oceanographic protocols described in the United States Department of Energy (DOE) Handbook
95 (1994), it is not difficult to achieve the JIS protocol. The JIS and DOE standard protocols allow
96 measurement errors of less than ± 0.07 and ± 0.003 , respectively, for the glass electrode method, and
97 the DOE protocol demands a precision of ± 0.001 for the spectrophotometric method. Measurements
98 are generally made with the higher-quality spectrophotometric method during major oceanographic
99 studies (e.g. Midorikawa et al. 2010).

100 Regardless of any shortcomings, the WPCL coastal monitoring program in Japan includes more
101 than 2000 monitoring sites that cover most parts of the coastline (Fig. 1), so the dataset provides the
102 opportunity to estimate the overall trend in pH in Japanese coastal areas and the regional variability in
103 the trends from data of known precision. Suitable analytical methods could make up for these
104 shortcomings of the WPCL dataset. In this study, we focused on the general characteristics of the
105 overall pH trends at the all monitoring sites rather than examining the trend in pH at each site in detail,
106 after carefully considering the accuracy of the dataset.

107 In the present study, we examined the $\text{pH}_{\text{insitu}}$ trends in surface coastal seawater from data measured
108 as part of WPCL monitoring programs. We then examined the trends at specific locations. The
109 remainder of this manuscript is organized as follows: the data and methods are described in Section 2,
110 and trends in $\text{pH}_{\text{insitu}}$ are presented in Section 3, the results are discussed in Section 4, and the
111 concluding remarks are provided in Section 5.

112

113 2. Materials and Methods

114 2.1 Water Pollution Control Law (WPCL) monitoring data

115 Data for several environmental variables, including $\text{pH}_{\text{insitu}}$, and the associated metadata, are
116 available on the website of the National Institute for Environmental Studies (NIES)
117 (www.nies.go.jp/igreen; http://www.nies.go.jp/igreen/md_down.html). We downloaded $\text{pH}_{\text{insitu}}$ data
118 from 1978 to 2009 for the trend analysis. We also downloaded temperature (T) and total nitrogen (TN)

119 data that were measured at the same sites as the $\text{pH}_{\text{insitu}}$ data for the same time period (data for T and
120 TN were available from 1981 to 1995), to check the quality of the $\text{pH}_{\text{insitu}}$ data (Section 2.2), and to
121 discuss which coastal processes influenced the $\text{pH}_{\text{insitu}}$ (Section 4.2).

122 The data were collected by the Regional Development Bureau of the Ministry of Land,
123 Infrastructure, Transport and Tourism, and the Ministry of the Environment under the WPCL
124 monitoring program. Monitoring protocols (sampling frequencies, locations, and methods) are outlined
125 in the program guidelines (NIES 2018; Ministry of Environment (MOE) 2018) written in Japanese,
126 and we have provided a summary of these protocols in this manuscript.

127 Monitoring is carried out at 1481 sites along the Japanese coasts, as shown in Figure 1a. While
128 most sites are in coastal sea areas, up to 10% are in estuaries. At each monitoring site, basic surveys
129 were carried out between 4 and 40 times a year, depending on the site. Information on the sampling
130 frequency at the monitoring sites is presented in Table 1. During basic surveys, water samples were
131 collected from 0.5 and 2.0 m below the surface at all sites; at sites where the bottom depths were
132 greater than 10 m, a further sample was collected from a depth of 10 m at about 13–15% of the sites.
133 Water samples were collected four times a day to cover diurnal variation. At sites where the variation
134 in the daily pH was large, samples were also collected over a period of one day at 2-hourly intervals
135 (ca. 13 times a day) at least twice a year to check the adequacy of the basic water sampling protocol.

136 The pH for each water sample was measured in accordance with the Japanese Industrial Standard
137 protocol JIS Z 8802 (2011), which is equivalent to ISO10523

138 (<https://www.iso.org/standard/51994.html>). The pH was measured by glass electrode calibrated by
139 NBS standard buffers. The electrode and pH meter had to produce measurements that were repeatable
140 to ± 0.05 . The pH was measured immediately after the water samples were collected, at the ambient
141 water temperature. The repeatability permitted in each measurement was ± 0.07 . The pH data were
142 collated by the environmental bureau of each prefectural government, which reported only annual
143 minimum and maximum pH values at each station to the MOE, because the original purpose of the
144 WPCL program was to monitor whether the annual variations in water properties (in this case pH)
145 were within ranges set by the national environmental quality standard. The published WPCL pH
146 dataset therefore contains only these annual minimum and maximum pH data in each year, reported
147 on the NBS pH scale ($\text{pH}_{\text{insitu}}$) and rounded to one decimal place. Water temperature data are also
148 available for each sampling event (http://www.nies.go.jp/igreen/md_down.html). Previous studies
149 have reported negative correlations between seasonal variations in pH and water temperature, mainly
150 because of changes in the dissociation equilibrium constant ($\text{H}_2\text{O} \leftrightarrow \text{H}^+ + \text{OH}^-$); the pH values were
151 lowest in summer and highest in winter, in both the open ocean (e.g. Bates et al. 2014) and coastal
152 seawater (e.g., Frankignoulle and Bouquegneau 1990; Byrne et al. 2013; Hagens et al. 2015; Challenger
153 et al. 2016). We therefore assumed that the minimum and maximum pH data coincided with the highest
154 and lowest temperatures, respectively (Fig. 2), and we used these data to calculate the pH_{25} (Section
155 4.2).

156 The monitoring operations were carried out by licensed operators as outlined in the annual plan of

157 the Regional Development Bureau of each prefecture. These specific licensed operators were retained
158 for the duration of the measurement period, which means that the same laboratories were always in
159 charge of collecting the data. This approach helps to prevent systematic errors that might arise both
160 between measurement facilities and over time, and ensures the datasets are accurate.

161

162 2.2 Quality control procedures and assessing the consistency of the WPCL monitoring data

163 We selected all the data for fixed sites in coastal seawater that had continuous time series from
164 1978 to 2009. There were 2463 regular and non-regular monitoring sites in 1978 and 2127 sites in
165 2009. While there were very few sites in some prefectures in Hokkaido and Tohoku, the monitoring
166 sites covered almost all the coastline in Japan (Fig. 1).

167 As explained in more detail later in this section, we applied a three-step quality control procedure.
168 We excluded 1) discontinuous time sequences, 2) time sequences that had extreme outliers in each year,
169 and 3) time sequences that included significant random errors, and which were only weakly correlated
170 with time sequences at adjacent sites.

171 When we excluded the sites that had discontinuous $\text{pH}_{\text{in situ}}$ time sequences from 1978 to 2009, 1481
172 sites remained (Fig. 1). We then excluded time sequences with outliers, defined as sites with data points
173 that were more than three standard deviations from the average of minimum and maximum $\text{pH}_{\text{in situ}}$
174 values for each year. After this step, 1127 sites remained (not shown). We calculated the trends in the
175 unbroken continuous time sequences of the minimum and maximum $\text{pH}_{\text{in situ}}$ data at each site with

176 linear regression (Fig. 3), and the slopes of the linear regression were taken as the minimum and
177 maximum $\text{pH}_{\text{insitu}}$ trends (e.g. Fig. 3). The linear regression trends might have been influenced by
178 random errors or variations at different temporal scales in the data for each site. To eliminate the
179 influence of these errors and variations as far as possible, we removed the data that had significant
180 random errors, defined as the time sequences for which the standard deviations of $\text{pH}_{\text{insitu}}$ exceeded the
181 average standard deviation of the $\text{pH}_{\text{insitu}}$ time sequences at the 1127 sites. After this step, 302 sites
182 remained (see Fig. 1b for site locations).

183 For the 302 sites, we evaluated whether the water temperature (Fig. 4a–b) and $\text{pH}_{\text{insitu}}$ (Fig. 4c–d)
184 were correlated at adjacent monitoring sites in the same prefecture (Fig. 4). At most of the stations, the
185 correlations between the temperatures at the site pairs were relatively strong, which indicates that the
186 temperature followed similar patterns over time at adjacent sites (Fig. 4a–b). The correlations tended
187 to be strong when the sites were close together, but gradually weakened with increasing distance
188 between sites. The $\text{pH}_{\text{insitu}}$ correlations followed a similar pattern (Fig. 4), which indicates that the
189 $\text{pH}_{\text{insitu}}$ and temperature data at adjacent monitoring sites varied in the same way. In other words, the
190 relative ratios of the measurement errors in $\text{pH}_{\text{insitu}}$ and the natural spatio-temporal variations at these
191 monitoring sites were similar to those for temperature. The absolute values of the correlation
192 coefficients for the $\text{pH}_{\text{insitu}}$ were slightly lower than those for temperature for each corresponding pair
193 of sites (Figs. 4 and 5), and might reflect the fact that $\text{pH}_{\text{insitu}}$, but not the water temperature, is subjected
194 to strong forcing by coastal biological processes, which causes the $\text{pH}_{\text{insitu}}$ to vary on the short-term.

195 The correlations between the minimum $\text{pH}_{\text{insitu}}$ data (Fig. 4c) were weaker than those for the maximum
196 $\text{pH}_{\text{insitu}}$ data (Fig. 4d) because the degree of biological forcing varied by season and was stronger in
197 summer when the $\text{pH}_{\text{insitu}}$ was at a minimum and weaker in the winter when the $\text{pH}_{\text{insitu}}$ was at a
198 maximum. Despite the influence of biological processes on the $\text{pH}_{\text{insitu}}$, the correlation coefficients
199 remained high and were significant ($r=0.367$, $p<0.05$) at most of the monitoring sites, especially at
200 sites that were less than 5 km apart within the same prefecture, where the $\text{pH}_{\text{insitu}}$ followed similar
201 patterns. In the final step of the quality check procedure (step 3), we removed all the time sequences
202 with weak and insignificant correlations for temperature and $\text{pH}_{\text{insitu}}$ (Figs. 4 and 5). After this final
203 step, 289 sites remained.

204 As shown in Table 2, the correlations between temperature and $\text{pH}_{\text{insitu}}$ at sites within 15 km of
205 each other strengthened after steps 2 and 3, which suggests that the reliability of the dataset improved
206 at each step of the quality control. Also, the negative correlations between trends in $\text{pH}_{\text{insitu}}$ and TN
207 were enhanced after the quality control procedures (Table 3), as discussed in Section 4.3.2.

208 The monitoring in each prefecture is carried out by different licensed operators, decided by the
209 Regional Development Bureau in each prefecture. Inter-calibration measurements have not been
210 conducted between different licensed operators. Even though all the operators follow the same JIS
211 protocol, manual monitoring can introduce systematic errors into the data. Some adjacent monitoring
212 sites are close to each other but are managed by different operators, such as sites close to the boundaries
213 between Osaka and Hyogo (Fig. 6a), Hyogo and Okayama (Fig. 6b), Kagawa and Okayama (not

214 shown), and Kagawa and Ehime (not shown). The $\text{pH}_{\text{insitu}}$ time sequences for these site pairs were
215 generally similar, even though there were some deviations when compared with the time sequences
216 for adjacent sites within the same prefecture, monitored by the same operator (lines of the same color
217 in Fig. 6). The standard deviations of the $\text{pH}_{\text{insitu}}$ trends between these site pairs close to the boundaries
218 of Osaka and Hyogo, Hyogo and Okayama, Kagawa and Okayama, and Kagawa and Ehime were
219 0.0014, 0.0012, 0.0026, and 0.0017 yr^{-1} , respectively, and were smaller than the acceptable
220 measurement errors of the JIS standard protocols. We can therefore say that the measurements from
221 the different operators in different prefectures were consistent.

222

223 3. Results

224 3.1 Variations in $\text{pH}_{\text{insitu}}$ highlighted by regression analysis

225 The histograms of the calculated $\text{pH}_{\text{insitu}}$ trends (yr^{-1}), for the minimum and maximum $\text{pH}_{\text{insitu}}$ after
226 each quality control step, are shown in Fig. 7. The histogram in Fig. 7a–b shows the data for the 1481
227 sites (discontinuous sites excluded). The data for the 1127 sites from step 2 (i.e., data without outliers)
228 are shown in Fig. 7c–d, and the data for the 289 sites from step 3 are shown in Fig. 7e–f (Section 2.2).
229 The number of sites decreased at each step of the quality control, but the shapes of the histograms were
230 generally similar for both the minimum and maximum pH trends. The total trends showed overall
231 normal distributions with a negative shift at all levels of quality control.

232 We detected both positive (basification) and negative (acidification) trends, which contrasts with

233 the findings of other researchers who reported only negative trends (ocean acidification) in the open
234 ocean (Bates et al. 2014; Midorikawa et al. 2010; Olafsson et al. 2009; Wakita et al. 2017). The average
235 (\pm standard deviation) trends for the minimum and maximum $\text{pH}_{\text{insitu}}$ data were -0.0002 ± 0.0061 and
236 $-0.0023 \pm 0.0043 \text{ yr}^{-1}$ for the 1481 sites (Fig. 7a–b), and -0.0005 ± 0.0042 and $-0.0023 \pm 0.0036 \text{ yr}^{-1}$ for
237 the 1127 sites (Fig. 7c–d), respectively. The average trends for the minimum and maximum $\text{pH}_{\text{insitu}}$
238 data for the 289 sites that remained after step 3 were -0.0014 ± 0.0033 and $-0.0024 \pm 0.0042 \text{ yr}^{-1}$,
239 respectively (Fig. 7e–f).

240 The negative trends were relatively weak for the minimum $\text{pH}_{\text{insitu}}$ data and relatively strong for
241 the maximum $\text{pH}_{\text{insitu}}$ data, but there was an overall tendency towards acidification. At the 289 sites,
242 there were 204 negative and 86 positive trends for the minimum $\text{pH}_{\text{insitu}}$ data and 217 and 72 negative
243 and positive trends for the maximum $\text{pH}_{\text{insitu}}$ data. This shows that, for the minimum $\text{pH}_{\text{insitu}}$ data, there
244 were acidification and basification trends at 70% and 30% of the monitoring sites, respectively, and at
245 75% and 25% for the maximum $\text{pH}_{\text{insitu}}$ data, respectively.

246

247 3.2 Local patterns in acidification and basification

248 We examined the $\text{pH}_{\text{insitu}}$ trends for the 289 sites for local patterns in acidification and basification
249 (Section 2.2) and found that the trends seemed to be randomly distributed. For example, the values
250 were different at sites that were less than 50 km apart (Fig. 8). There are many monitoring sites in the
251 Seto Inland Sea and in Western Kyushu. The trends for the minimum and maximum $\text{pH}_{\text{insitu}}$ showed

252 both acidification and basification in the Seto Inland Sea (Fig. 8a–b, 8c–d). In the western part of
253 Kyushu, acidification dominated (Fig. 8a–b, 8c–d) with only basification in $\text{pH}_{\text{insitu}}$ at a few sites for
254 both the minimum and maximum $\text{pH}_{\text{insitu}}$ data (Fig. 8b, d). Figure 8a (b) and Figure 8c (d) are similar,
255 which suggests that, at most of the sites where we detected acidification and basification, the trend
256 directions were consistent for the minimum and maximum $\text{pH}_{\text{insitu}}$ (Fig. 8a–b, 8c–d).

257 By examining the average minimum and maximum $\text{pH}_{\text{insitu}}$ trends in each prefecture (Fig. 9a–b, d–e,
258 g–h, j–k), we found that, while the average values were slightly different, the trends in the averaged
259 values and the patterns in acidification and basification for both the minimum and maximum $\text{pH}_{\text{insitu}}$
260 were the same from north to south and from west to east. We also found acidification trends in most of
261 the prefectures with at least 17 sampling sites, namely Miyagi, Wakayama, Hyogo, Okayama,
262 Yamaguchi, Tokushima, Kagawa, Ehime, and Nagasaki (Figs. 1a and 9c, f, i, l). The average estimates
263 for the maximum $\text{pH}_{\text{insitu}}$ were larger than those for the minimum $\text{pH}_{\text{insitu}}$ in these prefectures.

264 We found more acidification trends for the minimum $\text{pH}_{\text{insitu}}$ in the southwestern prefectures of
265 Yamaguchi, Kagawa, Ehime, Hyogo, and Nagasaki than in the northeastern prefecture of Miyagi (Fig.
266 9a, d, g, i) (see Fig. 1 for locations). The maximum and minimum $\text{pH}_{\text{insitu}}$ trends indicated basification
267 in Wakayama and Okayama prefectures (Fig. 9c). The trends in Osaka, Hyogo, Okayama, Hiroshima,
268 Yamaguchi, Kagawa, and Ehime prefectures (Fig. 1a) were different, even though they were all located
269 in the same part of the Seto Inland Sea (Fig. 9d–e). The trends in Hiroshima and Okayama, within the
270 Seto Inland Sea, were weaker than those in Hyogo, Yamaguchi, Kagawa, and Ehime, which were

271 outside the sea (Fig. 9d–e). The $\text{pH}_{\text{insitu}}$ trend values indicated relatively strong acidification at a rate
272 of -0.0025 yr^{-1} in Niigata in the Japan Sea (Fig. 9j–l) but there were fewer than the threshold of 17
273 monitoring sites in the prefectures.

274

275 4. Discussion

276 4.1 Statistical evaluation of our estimated overall trends

277 The JIS Z8802 (2011) allows a measurement error of ± 0.07 and this treatment further enhanced the
278 uncertainty of the published data to ± 0.1 . The uncertainty of the slope of the linear regression line (σ_{β})
279 is estimated with the following equation (e.g., Luenberger 1969):

$$280 \quad \sigma_{\beta} = \left\{ \sigma_y^2 / \sum (x_i - [x])^2 \right\}^{1/2} \quad (1)$$

281 where σ_y^2 is the theoretical variance in a pH value caused by the measurement error (in this case, 0.1^2
282 = 0.01); and x_i and $[x]$ represent the year and the year averaged for all data at a station, respectively.

283 In the WPCL dataset, there are generally 32 data points for each station (for every year from 1978 to
284 2009), spaced at consistent intervals. In this case, $\sum (x_i - [x])^2$ becomes 2728 and σ_{β} becomes 0.0020
285 yr^{-1} , which is the threshold of significance for the pH trend. This means that our estimated trends
286 included standard deviations that were less than 0.0020 yr^{-1} , and, if there were no trends, a histogram
287 of the pH trends should be normally distributed with an average and standard deviation (σ_{β}) of 0.0000
288 and 0.0020 yr^{-1} , respectively (Fig. 7). The average trend in the maximum $\text{pH}_{\text{insitu}}$, however, shifted
289 from zero in a negative direction at a rate of more than 0.0020 yr^{-1} for all three scenarios (Fig. 7b, d,

290 f). This result implies that, averaged over the whole country, the Japanese coast was acidified in winter
291 to a degree that could be detected from the historical WPCL pH data, even with an uncertainty of ± 0.1 .
292 The observed standard deviation for the maximum $\text{pH}_{\text{insitu}}$ was also larger than the expected value of
293 0.0020 yr^{-1} because of local variations in the pH trends. The average shift in the minimum $\text{pH}_{\text{insitu}}$ data
294 was smaller than 0.0020 yr^{-1} , but all three scenarios showed negative shifts in the average minimum
295 $\text{pH}_{\text{insitu}}$ value (Fig. 7a, c, e).

296 We used Welch's *t* test to assess the direction of the average minimum and maximum $\text{pH}_{\text{insitu}}$ trends.
297 For our null hypothesis, we assumed that the population of the trends with an average of -0.0014 yr^{-1}
298 (-0.0024 yr^{-1}) and a standard deviation of 0.0033 yr^{-1} (0.0042 yr^{-1}) was sampled from a population of
299 the minimum (maximum) $\text{pH}_{\text{insitu}}$ trends with an average trend of 0.0000 yr^{-1} and a standard deviation
300 of 0.0020 yr^{-1} . When the sample size was 289, the *t*-values and the degrees of freedom were 8.7 (6.2)
301 and 412.2 (474.4), respectively. Since the *p* value was less than 0.001, the null hypothesis was rejected.
302 Welch's *t* test confirmed that the average trends for both the minimum and maximum $\text{pH}_{\text{insitu}}$ data were
303 negative.

304 We also applied a paired *t* test to determine whether the two trends calculated from the averaged
305 minimum and maximum $\text{pH}_{\text{insitu}}$ data were significantly different. The population mean and the sample
306 size were 0.0 and 289, respectively. The *t* value of 4.64 (with 288 degrees of freedom) shows that the
307 null hypothesis was rejected, with the paired *t* test thus indicating that the two trends calculated from
308 the averaged minimum and maximum $\text{pH}_{\text{insitu}}$ data were significantly different.

309

310 4.2 Effects of sampling depth

311 The WPCL dataset did not discriminate between surface (0.5–2 m) and subsurface (10 m) data when
312 calculating the annual maximum and minimum $\text{pH}_{\text{insitu}}$, although monitoring depths were fixed
313 throughout the monitoring period at all the sites. We estimated the percentage possibility that samples
314 were collected at 10 m depth for the quality-controlled datasets with 1481, 1127, and 289 sites,
315 assuming that pH values were measured at the same depth as temperature, and found that samples
316 might have been collected at a depth of 10 m at 13%, 13%, and 15% of the 1481, 1127, and 289 sites,
317 respectively.

318 Usually the pH is lower in subsurface water than in surface water, as primary production decreases
319 and increases the DIC concentrations in surface and subsurface water, respectively, because of
320 decomposition when Particulate Organic Carbon (POC) is produced by primary producers. We
321 therefore speculate that the annual maximum pH includes very little data from a depth of 10 m, and so
322 this value does represent the winter pH of surface waters. In contrast, the annual minimum pH was
323 somewhat difficult to interpret, as it may have contained data from 10 m at some monitoring sites but
324 only surface data at other sites shallower than 10 m.

325 Results of statistical analysis (Section 4.1) confirm that the trends in minimum and maximum $\text{pH}_{\text{insitu}}$
326 data tended to be negative in the seawater around Japan. The negative tendency of the annual maximum
327 $\text{pH}_{\text{insitu}}$ trends may imply a trend of overall acidification in winter in surface waters around the Japanese

328 coasts, but the pattern in the annual minimum $\text{pH}_{\text{insitu}}$ trends was difficult to interpret. Nevertheless,
329 the annual minimum $\text{pH}_{\text{insitu}}$ trends were, as for the annual maximum $\text{pH}_{\text{insitu}}$, also negative (Section
330 3.1) and the trends in the annual minimum $\text{pH}_{\text{insitu}}$ and in the annual maximum $\text{pH}_{\text{insitu}}$ showed similar
331 patterns locally (Section 3.2), which indicate that long-term variations in the annual minimum and
332 maximum $\text{pH}_{\text{insitu}}$ were controlled by the same forcing, so that the $\text{pH}_{\text{insitu}}$ trends changed in the same
333 direction at both surface and subsurface. Global phenomena such as increases in atmospheric CO_2 and
334 warming of surface water temperatures may cause these forcings.

335

336 4.3 Possible influences on the $\text{pH}_{\text{insitu}}$ trends in coastal seawater

337 To facilitate our discussion of the factors that influenced the $\text{pH}_{\text{insitu}}$ trends further, we used the
338 conceptual models of acidification and basification in coastal seawater of Sunda and Cai (2012) and
339 Duarte et al. (2013), as follows:

$$340 \quad \text{pH}_{\text{insitu}} = \text{Function} (\text{D} (\text{T}), \text{DIC} (\text{Air } \text{CO}_2, \text{B} (\text{T}, \text{N})), \text{Alk}(\text{S})) \quad (2)$$

341 The $\text{pH}_{\text{insitu}}$ varies with the ambient temperature (T) on seasonal, inter-annual, and decadal time scales
342 mainly because of changes in the water dissociation constant in equilibrium (D; $\text{H}_2\text{O} \leftrightarrow \text{H}^+ + \text{OH}^-$).
343 Changes in dissolved inorganic carbon (DIC), alkalinity (Alk), and salinity (S) also affect the $\text{pH}_{\text{insitu}}$
344 trends. The solubility pump, which is controlled mainly by the atmospheric CO_2 concentration (Air
345 CO_2 ; $\text{CO}_2 + \text{H}_2\text{O} \leftrightarrow \text{H}^+ + \text{HCO}_3^-$), affects DIC, and ocean acidification occurs when the Air CO_2
346 increases. Dissolved organic carbon can also be affected by biological processes (B) that depend on

347 the ambient temperature (T) and the nutrient loading (N). There are contrasting relationships between
348 DIC and N in heterotrophic and autotrophic oceans. In the waters where organic decomposition is
349 dominated by primary productivity (i.e., autotrophic water), increases in N will enhance primary
350 production and cause DIC to decrease, raising pH. When N increases in the waters adjoining this
351 autotrophic water mass (for example, subsurface waters), POC transport from the autotrophic water
352 mass will also increase, and DIC will increase as POC decomposes (i.e., heterotrophic water), causing
353 acidification (e.g., Sunda and Cai 2012; Duarte et al., 2013). Alkalinity (Alk) generally varies with
354 salinity (S) in coastal oceans and may also affect the $\text{pH}_{\text{insitu}}$ trend.

355 The DIC process (Air CO_2) of ocean acidification shown in equation 2 generally occurred at all
356 monitoring sites when the Air CO_2 concentrations were horizontally uniform, resulting in overall
357 negative trends in minimum and maximum $\text{pH}_{\text{insitu}}$. There was also an overall warming trend in D (T)
358 in Japanese coastal areas, which may have affected the observed $\text{pH}_{\text{insitu}}$ trend. Both the DIC (Air CO_2)
359 and D (T) may be associated with global processes of warming and ocean acidification, which were
360 triggered by the increases in CO_2 concentrations in the global atmosphere.

361 It is difficult to observe general trends in both DIC (B (T, N)) and Alk (S) at all monitoring sites,
362 because there were no common trends in the factors that control these variables (e.g., salinity of coastal
363 water and terrestrial nutrient loadings) around the Japanese coast in this dataset. The WPCL data
364 should contain stations with both autotrophic and heterotrophic properties (Smith and Hollibaugh,
365 1992), which further obscures the influence of DIC (B (T, N)) on the overall $\text{pH}_{\text{insitu}}$ trend, as the same

366 trend in B (T, N) leads to opposite trends in DIC (B (T, N) in autotrophic and heterotrophic ocean
367 waters (Duarte et al., 2013). The wide variations in DIC (B (T, N)) and Alk (S) between regions might
368 have caused the regional differences in $\text{pH}_{\text{insitu}}$ trends among stations, contributing to relatively large
369 standard deviations in both the minimum and maximum $\text{pH}_{\text{insitu}}$ trends (Fig. 7).

370 We discuss the effects of global processes on the overall average pH trends are discussed in Section
371 4.3.1. The relationships between local effects and regional differences are discussed in Section 4.3.2.

372

373 4.3.1 Global effects on $\text{pH}_{\text{insitu}}$ trends

374 Our analysis was based on $\text{pH}_{\text{insitu}}$ data, so differences observed in trends may reflect long-term
375 changes in water temperature that affected the dissociation constant (process D (T) in equation 2) or
376 changes in the coastal carbon cycle, including absorption of anthropogenic carbon by the solubility
377 pump (process DIC (Air CO_2) in equation 2). Some of the effects of D (T) and DIC (Air CO_2) driven
378 by global warming and ocean acidification may have affected all monitoring sites, and may have
379 contributed to the negative shifts in trend distributions.

380 To evaluate the direct thermal effects related to process D (T) in equation 2, we estimated the pH
381 values normalized to 25°C (pH_{25}), assuming that the minimum (maximum) $\text{pH}_{\text{insitu}}$ and highest (lowest)
382 temperature and other parameters were measured at the same time. By assuming the other parameters
383 that affected the pH calculation in the CO_2sys (Lewis and Wallace 1998, csys.m), such as salinity,
384 DIC, and alkalinity, did not change (these parameters are not measured as part of the WPCL program),

385 we used the method of Lui and Chen (2017) to calculate the pH_{25} , as follows:

$$386 \quad \text{pH}_{25} = -\text{pH}_{\text{insitu}} + a_1(T - 25 \text{ }^\circ\text{C}), \quad (3)$$

387 where a_1 was set to -0.015 and T was the observed temperature.

388 The distributions of the trends in pH_{25} after applying equation 3 are shown in Fig. 10. The minimum
389 and maximum pH_{25} data were normally distributed, meaning that the distributions of the $\text{pH}_{\text{insitu}}$ trends
390 were maintained after applying equation 3 (Fig. 7e, f). The averages (\pm standard deviations) of the
391 minimum and maximum pH_{25} trends were -0.0010 ± 0.0032 and $-0.0014 \pm 0.0041 \text{ yr}^{-1}$, respectively.
392 The averaged trends are consistent with those reported by Midorikawa et al. (2010), who calculated
393 that the pH_{25} decreased at rates of $-0.0013 \pm 0.0005 \text{ yr}^{-1}$ and $-0.0018 \pm 0.0002 \text{ yr}^{-1}$ in summer and
394 winter from 1983 to 2007 along the 137°E line of longitude in the north Pacific. The asymmetry of
395 pH_{25} trends between the minimum and maximum estimates may be related to seasonal variations in
396 pCO_2 and associated asymmetric responses of the air–sea CO_2 flux (Landschutzer et al., 2018;
397 Fassbender et al., 2018).

398 We used Welch’s t test to assess the direction of the averages of minimum and maximum pH_{25}
399 trends. The p value was less than 0.001, so the null hypothesis was rejected again. The results of the t
400 test confirm that the average trends for both the minimum and maximum pH_{25} data were also negative,
401 suggesting that the DIC (AirCO_2) effect (i.e., ocean acidification) caused the negative shifts in the
402 distribution of the trend for the pH normalized to 25°C .

403 The pH_{25} and $\text{pH}_{\text{insitu}}$ trends from north to south and from west to east were similar among the

404 prefectures (Fig. 11), except in Miyagi and Tokushima. The trends in the minimum $\text{pH}_{\text{insitu}}$ and summer
405 pH_{25} were quite similar, but the minimum and maximum $\text{pH}_{\text{insitu}}$ trends tended to be more negative (by
406 about -0.0010 yr^{-1}) than the corresponding pH_{25} trends, especially in Wakayama, Hiroshima, Kagawa,
407 and Ehime, which met the threshold number of sampling sites.

408 The average highest temperatures observed at the minimum $\text{pH}_{\text{insitu}}$ were close to $25 \text{ }^{\circ}\text{C}$ in the
409 regions south of Chiba prefecture (Figs. 1 and 12a–d), so the normalization at $25 \text{ }^{\circ}\text{C}$ did not have much
410 effect on the minimum pH_{25} in the southern prefectures. In contrast, the maximum $\text{pH}_{\text{insitu}}$ values were
411 observed at temperatures that were more than $10 \text{ }^{\circ}\text{C}$ lower than $25 \text{ }^{\circ}\text{C}$, so the normalization worked
412 well on the winter data. We estimated the temperature trends from the highest and lowest temperatures
413 at the 289 sites that remained after quality control step 3. The trends in the highest and lowest
414 temperatures generally indicated warming, with an average and standard deviation of 0.021 ± 0.040 and
415 $0.047 \pm 0.036 \text{ deg. yr}^{-1}$, respectively (Fig. 13). Estimations from the CO2sys indicate that these warming
416 trends influenced the pH values and were related to the changes of -0.0004 and -0.0010 yr^{-1} in the
417 pH trends in summer and winter, respectively (Fig. 7e–f and 10a–b).

418 We estimated that the $\text{pH}_{\text{insitu}}$ would change from 8.0150 to 8.0147 in summer and from 8.2568 to
419 8.2560 in winter, for temperature changes from 25.00 to $25.02 \text{ }^{\circ}\text{C}$, and from 10.00 ° to $10.04 \text{ }^{\circ}\text{C}$,
420 respectively, for a salinity of 34, DIC of $1900 \text{ millimol m}^{-3}$, and alkalinity of $2200 \text{ millimol m}^{-3}$. The
421 differences between the $\text{pH}_{\text{insitu}}$ and the corresponding pH_{25} trends in summer (-0.0004 yr^{-1}) and winter
422 (-0.0010 yr^{-1}) can be partly explained by the difference between the decrease in the pH trends in

423 summer (-0.0003 yr^{-1}) and winter (-0.0005 yr^{-1}) (Fig. 7e–f) arising from the thermal effects.

424

425 4.3.2 Local effects on $\text{pH}_{\text{insitu}}$ trends

426 We found regional differences in the $\text{pH}_{\text{insitu}}$ values (e.g. Fig. 6) and $\text{pH}_{\text{insitu}}$ trends (Figs. 8–9). The
427 negative $\text{pH}_{\text{insitu}}$ trends (acidification) were more significant in southwestern Japan than in northeastern
428 Japan, especially for the minimum $\text{pH}_{\text{insitu}}$ data (Fig. 9 and Section 3.2). The JMA (2008, 2018)
429 reported that over the past 100 years, the increase in water temperature in western Japan was $\sim 1.30 \text{ }^\circ\text{C}$
430 greater than that in northeastern Japan.

431 We used CO2sys (Lewis and Wallace 1998) to predict how $\text{pH}_{\text{insitu}}$ would change under a
432 temperature difference of $0.01 \text{ }^\circ\text{C yr}^{-1}$ between the northeastern and southwestern areas, and found
433 that pH decreased by $0.0002 (0.0002) \text{ yr}^{-1}$ when the temperature changed from 10.00 to $10.01 \text{ }^\circ\text{C}$ (25.0
434 to $25.01 \text{ }^\circ\text{C}$), assuming a salinity of 34, DIC of $1900 \text{ millimol/m}^3$, and alkalinity of $2200 \text{ millimol/m}^3$.
435 The contrasting trends in the northeast and southwest can be also partly explained by the difference in
436 warming trends (process D (T) in equation 2).

437 The summer $\text{pH}_{\text{insitu}}$ is affected by ocean uptake of CO_2 (process DIC; Bates et al., 2012; Bates
438 2014) through long-term changes in biological activity (Cai et al., 2011; Sunda and Cai 2012; Duarte
439 et al., 2013; Yamamoto-Kawai et al., 2015) as well as the effect of changes in the dissociation constant.
440 The responses of $\text{pH}_{\text{insitu}}$ to changes in marine productivity are, however, complicated.

441 Previous studies have reported that nutrient loadings in Japan have decreased over recent decades

442 (e.g., Yamamoto-Kawai et al. 2015; Kamohara et al. 2018; Nakai et al. 2018), with variable effects on
443 summer $\text{pH}_{\text{insitu}}$ in coastal seawater. TN was monitored for a shorter period than $\text{pH}_{\text{insitu}}$ (1995 to 2009).
444 We assumed that the TN was mainly dissolved inorganic nitrogen and determined the correlations
445 between TN and the minimum and maximum $\text{pH}_{\text{insitu}}$ trends (Fig. 14). There were significant negative
446 correlations between TN and the minimum (-0.30) and maximum (-0.29) $\text{pH}_{\text{insitu}}$. These correlations
447 imply that the conditions in most of the monitoring areas of the WPCL programs were heterotrophic.
448 The results also imply that recent decreases in TN loadings partly offset anthropogenic CO_2 -induced
449 decreases in pH in coastal seawater. However, we should also be careful when interpreting these results,
450 as this may be a result of simultaneous progress in independent two phenomena (i.e., anthropogenic
451 carbon uptake from the ocean and decreases in TN loadings in Japan).

452 Nakai et al. (2018) reported that nutrient loadings decreased in the most parts of the Seto Inland Sea
453 from 1981 to 2010, but that several areas remained eutrophic. Because of geographical variations in
454 nutrient loadings and the uneven distribution of autotrophic and heterotrophic water areas, there are
455 significant spatial variations in pH trends in the Seto Inland Sea (Fig. 8). The pH trends in coastal areas
456 of western Kyushu, where the anthropogenic nutrient loadings are relatively low, therefore reflect the
457 decreases in nutrient discharges, resulting in variations between regions (e.g., Nakai et al. 2018;
458 Yamamoto and Hanazato 2015; Tsuchiya et al., 2018). Several cities in this area have introduced
459 advanced sewage treatment to prevent eutrophication in coastal seawater (Nakai et al. 2018;
460 Yamamoto and Hanazato 2015).

461 Regional variations in coastal alkalinity along with salinity might be related to changes in land use
462 and might affect the trends (process Alk(S) in equation 2). Taguchi et al. (2009) measured alkalinity in
463 the surface waters of Ise, Tokyo, and Osaka bays between 2007 and 2009, and reported that total
464 alkalinity was highly correlated with salinity in each bay. For a temperature, salinity, dissolved carbon,
465 and alkalinity of 25.00 °C, 35, 1900 millimol m⁻³, and 2300 millimol m⁻³, respectively, pH_{insitu} (=
466 pH₂₅) was estimated at 8.1416 using the CO₂sys (Lewis and Wallace 1998). By changing the salinity
467 and alkalinity to 34 and 2200 millimol m⁻³, respectively, pH_{insitu} (= pH₂₅) decreased by 0.0081 to
468 8.0150. This shows that the pH could deviate significantly from average trends if the inputs of alkaline
469 compounds are changed; consequently, some of our pH trends could have been affected by changing
470 discharge from different land-use types.

471 Regional differences in pH_{insitu} trends in coastal seawater might be caused by ocean pollution. The
472 speciation and bioavailability of heavy metals change in acidic waters, causing an increase in the
473 biotoxicity of the metals (Zeng et al. 2015; Lacoue-Labarthe et al. 2009; Pascal et al. 2010; Cambell
474 et al. 2014). The rates at which marine organisms photosynthesize and respire in ocean waters decrease
475 and increase, respectively, in water polluted with heavy metals and oils (process DIC in equation 2)
476 because of biotoxicity and eutrophication, thereby resulting in acidification (Hing et al. 2011; Huang
477 et al. 2011; Gilde and Pinckney 2012).

478

479

480 5. Conclusions

481 We estimated the long-term trends in $\text{pH}_{\text{insitu}}$ in Japanese coastal seawater and examined how the
482 trends varied regionally. The long-term $\text{pH}_{\text{insitu}}$ data show highly variable trends, although ocean
483 acidification has generally intensified in Japanese coastal seawater. We found that the annual
484 maximum $\text{pH}_{\text{insitu}}$ at each station, which generally represents the pH of surface waters in winter, had
485 decreased at 75% of the sites and had increased at the remaining 25% of sites. The temporal trend in
486 the annual minimum $\text{pH}_{\text{insitu}}$, which generally represents the summer pH in subsurface water at each
487 site, was also similar, but it was relatively difficult to interpret the trends of annual minimum $\text{pH}_{\text{insitu}}$
488 because the sampling depths differed from station to station. The average rate of decrease in the annual
489 maximum $\text{pH}_{\text{insitu}}$ was -0.0024 yr^{-1} , with relatively large deviations from the average value. Detailed
490 analysis suggests that the decrease in the pH was partly caused by warming of Japanese surface coastal
491 seawater in winter. However, the distributions of the trend in pH normalized to 25°C also showed
492 negative shifts, suggesting that anthropogenic DIC was also increasing in Japanese coastal seawater.

493 There were striking spatial variations in the $\text{pH}_{\text{insitu}}$ trends. Correlations among the $\text{pH}_{\text{insitu}}$ time
494 series at different sites revealed that the high variability in the $\text{pH}_{\text{insitu}}$ trends was not caused by
495 analytical errors in the data but reflected the large spatial variability in the physical and chemical
496 characteristics of coastal environments, such as water temperature, nutrient loadings, and
497 autotrophic/heterotrophic conditions. While there was a general tendency towards coastal acidification,
498 there were positive trends in $\text{pH}_{\text{insitu}}$ at 25%–30% of the monitoring sites, indicating basification, which

499 suggests that the coastal environment might not be completely devastated by acidification. If we can
500 manage the coastal environment effectively (e.g., control nutrient loadings and
501 autotrophic/heterotrophic conditions), we might be able to limit, or even reverse, acidification in coastal
502 areas.

503

504 Acknowledgments

505 We thank the scientists, captain, officers, and personnel of the National Institute for Environmental
506 Studies, Regional Development Bureau of the Ministry of Land, Infrastructure, Transport and Tourism,
507 who contributed to this study. We acknowledge financial support from the Sasakawa Peace Foundation
508 of the Ocean Policy Research Institute. We also appreciate discussions with members of the
509 Environmental Variability Prediction and Application Research Group of the Japanese Agency for
510 Marine-Earth Science and Technology. Suggestions by two reviewers helped us to improve an earlier
511 version of the manuscript.

512

513 References

- 514 Bates, N. R.: Interannual variability of the ocean CO₂ sink in the subtropical gyre of the North Atlantic
515 Ocean over the last 2 decades, *J. Geophys. Res.* 112, C09013, doi:10.1029/2006JC003759, 2007.
- 516 Bates, N. R.: Multi-decadal uptake of carbon dioxide into subtropical mode waters of the North
517 Atlantic Ocean. *Biogeosciences* 9:2, 649–2, 659, <http://dx.doi.org/10.5194/bg-9-2649-2012>, 2012.
- 518 Bates, N. R., Astor, Y. M., Church, M. J., Currie, K., Dore, J. E., Gonzalez-Davila, M., Lorenzoni, L.,
519 Muller-Karger, F., Olafsson, J., and Santana-Casiano, J. M.: A time-series view of changing surface

520 ocean chemistry due to ocean uptake of anthropogenic CO₂ and ocean acidification, *Oceanography*,
521 27 (1):126–141, <http://dx.doi.org/10.5670/oceanog.2014.16>, 2014.

522 Bednarsek, N., Tarling, G. A., Bekker, D. C. E., Fielding, S., Jones, E. M., Venables, H. J., Ward, P.,
523 Kuzirian, A., Leze, B., Feely, R. A., and Murphy, E. J.: Extensive dissolution of live pteropods in
524 the Southern Ocean, *Nature Geoscience Letter*, 5, 881–885, doi: 10.1038/NGEO1635, 2012.

525 Bednarsek, N., Feely, R. A., Reum, J. C. P., Peterson, B., Menkel, J., Alin, S. R., and Hales, B.:
526 *Limacina helicina* shell dissolution as an indicator of declining habitat suitability due to ocean
527 acidification in the California Current Ecosystem, *Proc. R. Soc. B*, 281 20140123, doi:
528 10.1098/rspb.2014.0123, 2014.

529 Borges, A. V. and Gypen, N.: Carbonate chemistry in the coastal zone responds more strongly to
530 eutrophication than to ocean acidification, *Limnology and Oceanography* 55: 346–353, 2010.

531 Montagna, R.: Description and quantification of pteropod shell dissolution: a sensitive bioindicator of
532 ocean acidification, *Global Change Biology*, 18, 2378–2388, doi: 10.1111/j.1365–2486.2012.02668,
533 2012.

534 Byrne, M., Lamare, M., Winter, D., Dworjanyn, S. A., and Uthicke, S.: The stunting effect of a high
535 CO₂ ocean on calcification and development in the urchin larvae, a synthesis from the tropics to the
536 poles, *Philosophical Transactions of the Royal Society B*, 368, 20120439. Doi:
537 10.1098/rstb.2012.0439, 2013.

538 Cai, W., Hu, X., Huang, W., Murell, M. C., Lehrter, J. C., Lohrenz, S. E., Chou, W., Zhai, W.,

539 Hollibaugh, J. T., Wang, Y., Zhao, P., Guo, X., Gundersen, K., Dai, M., and Gong, G.: Acidification
540 of subsurface coastal waters enhanced by eutrophication, *Nature Geoscience*, 4, 766–700, 2011.

541 Campbell, A. L., Mangan, S., Ellis, R. P., and Lewis, C.: Ocean acidification increases copper toxicity
542 to the early life history stages of the polychaete *arenicola marina* in artificial seawater, *Environ. Sci.*
543 *Technol.* 48, 9745–9753, 2014.

544 Challenger, R. C., Robbins, L. L., and McClintock, J. B.: Variability of the carbonate chemistry in a
545 shallow, seagrass-dominated ecosystem: implications for ocean acidification experiments, *Marine*
546 *and Freshwater Research*, 67, 163–172. Doi:10.1071/MF14219, 2016.

547 DOE (United States Department of Energy): Handbook of methods for the analysis of the various
548 parameters of the carbon dioxide system in sea water; ver. 2, edited by A. G. Dickson and C. Goyet,
549 ORNL/CDIAC-74, 1994.

550 Dore, J. E., Lukus, R., Sadler, D. W., Church, M. J. and Karl, D. M.: Physical and biogeochemical
551 modulation of ocean acidification in the central North Pacific, *Proc. Natl. Acad. Sci.* 106, 12 235–12
552 240, 2009.

553 Doney, S.C., Fabry, V. J., Freely, A., and Kleypas, J. A.: Ocean acidification: The other CO₂ program,
554 *Annu. Rev. Mar. Sci.*, 1, 169–192, 2009.

555 Duarte, C. M., Hendriks, I. E., Moore, T. S., Olsen, Y. S., Steckbauer, A., Ramajo, L., Carstensen, J.,
556 Trotter, J. A., and McCullough, M.: Is ocean acidification an open ocean syndrome? Understanding

557 anthropogenic impacts in seawater pH, *Estuaries and Coasts* 36, 221–236. doi:10.1007/s12237-013-
558 9594-3, 2013.

559 Fassbender J. A., Rodgers B. K., Palevsky I. H., and Sabine L. C.: Seasonal asymmetry in the evolution
560 of surface ocean pCO₂ and pH thermodynamic drivers and the influence on sea-air CO₂ flux, *Global
561 Biogeochemical Cycles*, 32, 11476–1497, 2018.

562 Frankignoulle, M., and Bouquegneau, J. M.: Daily and yearly variations of total inorganic carbon in a
563 productive coastal area, *Estuarine, Coastal and Shelf Science* 30, 79–89, 1990.

564 Gattuso, J. P., and Hansson, L.: *Ocean acidification*, Oxford Univ. Press, Oxford, 2011.

565 Glide, K., and Pinckney, J. L.: Sublethal effects of crude oil on the community structure of estuarine
566 phytoplankton, *Estuar. Coasts* 35, 853–861, 2012.

567 Gonzalez-Davila, M., Santana-Casiano, J. M., and Gonzalez-Davila, E. F.: Interannual variability of
568 the upper ocean carbon cycle in the northeast Atlantic Ocean, *Geophys. Res. Lett.* 34, L07608,
569 doi:10.1029/2006GL028145, 2007.

570 Hagens, M., Slomp, C. P., Meysman, F. J. R., Seitaj, D., Harlay, J., Borges, A. V., and Middelburg, J.
571 J.: Biogeochemical processes and buffering capacity concurrently affect acidification in a seasonally
572 hypoxic coastal marine basin, *Biogeosciences* 12, 1561–1583. Doi:10.5194/bg-12-1561-2015, 2015.

573 Hing, L. S., Ford, T., Finch, P., Crane, M., and Morrill, D.: Laboratory stimulation of oil-spill effects
574 on marine phytoplankton, *Aquat. Toxicol* 103, 32–37, 2011.

575 Huang, Y. J., Jiang, Z. G., Zeng, J. N., Chen, Q. Z., Zhao, Y. Q., Liao, Y. B., Shou, L., and Xu, X. Q.:
576 The chronic effects of oil pollution on marine phytoplankton in a subtropical bay, China. Environ.
577 Monit. Assess. 176, 517–530, 2011.

578 Intergovernmental Panel on Climate Change (IPCC): Climate Change 2013: The Physical Science
579 Basis. Contribution of Working Group I to the Fifth Assessment Report of the Intergovernmental
580 Panel on Climate Change, ed. Stocker, T. F., Qin, D., Plattner, Gian-Kasper., Tignor, M. M. B., Allen,
581 S. K., Boschung, J., Nauels, A., Zia Y., Bex, V., Midgley, P. M., 1–1535 pp. Cambridge,
582 UK: Cambridge University Press, Cambridge, United Kingdom and New York, NY, USA, 2013.

583 Japanese Industrial Standard Z8802 : <http://kikakurui.com/z8/Z8802-2011-01.html> (in Japanese), 2011.

584 Japanese Meteorological Agency :
585 [http://dl.ndl.go.jp/view/download/digidepo_3011050_po_synthesis.pdf?itemId=info%3Andljp%2F](http://dl.ndl.go.jp/view/download/digidepo_3011050_po_synthesis.pdf?itemId=info%3Andljp%2Fpid%2F3011050&contentNo=1&alternativeNo=&lang=en)
586 [pid%2F3011050&contentNo=1&alternativeNo=&lang=en](http://dl.ndl.go.jp/view/download/digidepo_3011050_po_synthesis.pdf?itemId=info%3Andljp%2Fpid%2F3011050&contentNo=1&alternativeNo=&lang=en), 2008.

587 Japanese Meteorological Agency :
588 https://www.data.jma.go.jp/kaiyou/data/shindan/a_1/japan_warm/japan_warm.html (in Japanese),
589 2018.

590 Kamohara, S., Takasu, Y., Yuguchi, M., Mima, N., and Yoshunari, A.: Nutrient decrease in Mikawa
591 Bay, Bulletin of Aichi Fisheries Research Institute 23, 30–32. (in Japanese), 2018.

592 Keeling, C. D., and Whorf, T. P.: Atmospheric CO₂ concentration–Manoa Loa Observatory, Hawaii,
593 1958-1997 (revised August 1998), ORNL NDP–001, Oak Ridge Natl. Lab. Oak Ridge, TN, 1998.

594 Lacou-Labarthe, T., Martin, S., Oberhansli, F., Teyssie, J. L., Jeffree, R., Gattuso, J. P., and
595 Bustamante, P.: Effects of increased pCO₂ and temperature on tracer element (Ag, Cd and Zn)
596 bioaccumulation in the eggs of the common cuttlefish, *Sepia officinalis*. *Biogeosciences* 6,
597 2561–2573, 2009.

598 Landschutzer P, Gruber N, Bakker C. E. D., Stemmler I, Six D. K.: Strengthening seasonal marine
599 CO₂ variations due to increasing atmospheric CO₂. *Nature Climate Change*, 8, 146–150, 2018.

600 Lemasson, A. J., Fletcher, S., Hall-Spence, J. M., and Knights, A. M.: Linking the biological impacts
601 of ocean acidification on oysters to changes in ecosystem services: A review, *Journal of Experimental*
602 *Marine Biology and Ecology*, 492, 49–62, 2017.

603 Lewis, E., and Wallace, D. W. R.: Program Developed for CO₂ System Calculations. ORNL/CDIAC-
604 105. Carbon Dioxide Information Analysis Center, Oak Ridge National Laboratory, U.S. Department
605 of Energy, Oak Ridge, Tennessee, 1998.

606 Luenberger, D. G.: Optimization by vector space methods, pp. 1-326, John Wiley & Sons, Inc., New
607 York, N.Y, 1969.

608 Lui, H., and Chen, A. C.: Reconciliation of pH₂₅ and pH_{insitu} acidification rates of the surface oceans:
609 A simple conversion using only in situ temperature, *Limnology and Oceanography: methods*, 15,
610 328–355, doi:1002/lom3.10170, 2017.

611 Midorikawa, T., Ishii, M., Sailto, S., Sasano, D., Kosugi, N., Motoi, T., Kamiya, H., Nakadate, A.,
612 Nemoto, K., and Inoue, H.: Decreasing pH trend estimated from 25-yr time series of carbonate

613 parameters in the western North Pacific, *Tellus*, 62B, 649–659, doi:
614 10.1111/j.1600–0889.2010.00474.x, 2010.

615 Ministry of the Environment: <http://www.env.go.jp/hourei/05/000140.html> (in Japanese), 2018.

616 Nakai, S., Soga, Y., Sekito, S., Umehara, S., Okuda, T., Ohno, M., Nishijima, W., and Asaoka, S.:
617 Historical changes in primary production in the Seto Inland Sea, Japan, after implementing
618 regulations to control the pollutant loads, *Water Policy* wp2018093. Doi:10.2166/wp.2018.093, 2018.

619 National Institute for Environmental Studies :
620 https://www.nies.go.jp/igreen/explain/water/content_w.html (in Japanese), 2018.

621 Olafsson, J., Olafsdottir, S. R., Benoit-Cattin, A., Danielsen, M., Arnarson, T. S., and Takahashi, T.:
622 Rate of Iceland Sea acidification from time series measurements, *Biogeosciences* 6:2, 661–2, 668,
623 <http://dx.doi.org/10.5194/bg-6-2661-2009>, 2009.

624 Pascal, P. Y., Fleeger, J. W., Galvez, F., and Carman, K. R.: The toxicological interaction between ocean
625 acidity and metals in coastal meiobenthic copepods, *Mar. Pollut. Bull*, 60, 2201–2208, 2010.

626 Sarmiento, J. L., and Gruber, N.: *Ocean Biogeochemical dynamics*, pp. 1-503, Princeton Univ. Press,
627 Princeton, New Jersey; Oxfordshire, United Kingdom, 2006.

628 Smith, S.V., and Hollibaugh, J. T.: Coastal metabolism and the oceanic carbon balance. *Review of*
629 *Geophysics*, 31, 75–89, 1993.

630 Sunda, W. G., and Cai, W. J.: Eutrophication induced CO₂-acidification of subsurface coastal waters:
631 interactive effects of temperature, salinity, and atmospheric pCO₂, *Environ. Sci. Technol.* 46,

632 10651–10659, 2012.

633 Taguchi, F., Fujiwara, T., Yamada, Y., Fujita, K., and Sugiyama, M.: Alkalinity in coastal seas around
634 Japan, *Bulletin on coastal oceanography*, Vol.47, No.1, 71–75, 2009.

635 Yamamoto-Kawai, M., Kawamura, N., Ono, T., Kosugi, N., Kubo, A., Ishii, M., and Kanda, J.: Calcium
636 carbonate saturation and ocean acidification in Tokyo Bay, Japan, *J. Oceanogr.* 71:427–439, doi
637 10.1007/s10872-015-0302-8, 2015.

638 Tsuchiya, K., Ehara, M., Yasunaga, Y., Nakagawa, Y., Hirahara, M., Kishi, M., Mizubayashi, K.,

639 Kuwahara, V. S., and Toda, T.: Seasonal and Spatial Variation of Nutrients in the Coastal Waters

640 of the Northern Goto Islands, Japan, *Bulletin on coastal oceanography*, 55, 125-138. (in

641 *Japanese*), 2018.

642 Yamamoto, T., and Hanazato, T.: Eutrophication problems of oceans and lakes, -fishes cannot live in

643 clean water, pp. 1–208, ChijinShokan Co. Ltd, ISBN978-4-8052-0885-4, (in Japanese), 2015.

644 Yara, Y., Vogli, M., Fujii, M., Yamano, H., Hauri, C., Steinacher, M., Gruber, N. and Yamano, Y. : Ocean

645 acidification limits temperature-induced poleward expansion of coral habitats around Japan,

646 *Biogeosciences*, 9, 4955–4968, doi : 10.5194/bg-9-4955-2012, 2012.

647 Zeng, X., Chen, X., and Zhuang, J.: The positive relationship between ocean acidification and pollution,

648 *Mar. Poll. Bull.*, 91, 14–21, 2015.

649 Wakita, M., Nagano, A., Fujiki, T., and Watanabe, S.: Slow acidification of the winter mixed layer in

650 the subarctic western North Pacific, *J. Geophys. Res. Oceans*, 122, 6923–6935,

651 doi:10.1002/2017JC013002, 2017.

652

653 Figure captions

654

655 Fig. 1 Coastal maps and monitoring sites in Japan. Red points in (a) indicate the fixed sites ($n = 1481$)
656 monitored by the Regional Development Bureau of the Ministry of Land, Infrastructure, Transport,
657 and Tourism, and the Ministry of the Environment (Japan) under the WCPL monitoring program. (b)
658 Monitoring sites that met the strictest criterion ($n = 302$).

659

660 Fig. 2 Distributions of the monthly number of data points (N) for (a) maximum and (b) minimum
661 temperatures collected in each prefecture from the 302 most reliable monitoring sites.

662

663 Fig. 3 Examples of (a) acidification (Kahoku Coast in Ishikawa) and (b) basification (Funakoshi Bay
664 in Iwate) trends at monitoring sites. Blue and red colors indicate the annual minimum and maximum
665 $\text{pH}_{\text{insitu}}$ data and their trends, respectively.

666

667 Fig. 4 Correlations of water temperature and $\text{pH}_{\text{insitu}}$ at adjacent monitoring sites in the same prefecture.
668 Thin lines denote significant correlations ($r = 0.12$, degrees of freedom = 283).

669

670 Fig. 5 Scatter plots of correlation coefficients for water temperature and $\text{pH}_{\text{insitu}}$ at adjacent monitoring
671 sites in the same prefecture. Fig. 5a shows the highest temperature and the minimum $\text{pH}_{\text{insitu}}$ and Fig.

672 5b shows the lowest temperature and maximum $\text{pH}_{\text{insitu}}$, respectively.

673

674 Fig. 6 Examples of time-series for annual minimum and maximum $\text{pH}_{\text{insitu}}$ data at adjacent monitoring
675 sites close to the boundaries between (a) Osaka and Hyogo and (b) Kagawa and Ehime. Lines of the
676 same color indicate data collected at the same site. Thin and bold lines indicate the annual minimum
677 and maximum $\text{pH}_{\text{insitu}}$ data, respectively, at each monitoring site. Site locations are included to the
678 right of each panel, with the text color corresponding to the colors in each panel.

679

680 Fig. 7 Histogram of pH trends, represented by $\Delta\text{pH}_{\text{insitu}}$, showing the slopes of the linear regression
681 lines for the annual minimum (left) and maximum (right) $\text{pH}_{\text{insitu}}$ data at each monitoring site. The
682 histograms in (a, b), (c, d), and (e, f) show three scenarios: (a, b) all 1481 available sites with
683 continuous records before quality control, (c, d) 1127 sites without outliers, and (e, f) 289 sites that
684 meet the strictest criterion.

685

686 Fig. 8 Distributions of long-term trends in $\text{pH}_{\text{insitu}}$ ($\Delta\text{pH}_{\text{insitu}}/\text{yr}$) in Japanese coastal seawater. The colors
687 indicate the ranges of acidification (a, c) and basification (b, d). (a, b) and (c, d) are linked to the data
688 used in Figs. 7e and 7f, respectively.

689

690 Fig. 9 (a–b, d–e, g–h, j–k) Average minimum and maximum $\text{pH}_{\text{insitu}}$ trends ($\Delta\text{pH}_{\text{insitu}}/\text{yr}$) in each

691 prefecture. These figures show each side of the Pacific (a–b), the Seto Inland Sea (d–e), the East
692 China Sea (g–h), and the Japan Sea (j–k). The prefecture names are arranged vertically from eastern
693 (northern) to western (southern) areas. Black shading indicate one standard deviation from the
694 average. (c, f, i, l) Number of monitoring sites in each prefecture and the thin dashed line is the
695 threshold value of 17 (i.e., the average number of monitoring sites in all prefectures). The prefectures
696 that meet the threshold are indicated in purple. The figure is based on the results shown in Figs. 7 (e,
697 f) and 8.

698

699 Fig. 10 Same as Fig. 7, but showing the pH_{25} trends at 289 sites (selected by quality control step 3).

700 The value of pH_{25} was estimated using the method of Lui and Chen (2017).

701

702 Fig. 11 (a–b, d–e, g–h, j–k) Same as Fig. 9, but showing the average estimated minimum and
703 maximum pH_{25} trends ($\Delta\text{pH}_{25}/\text{yr}$) for each prefecture. Red lines and points indicate the average
704 minimum and maximum $\text{pH}_{\text{insitu}}$ trends shown in Fig. 9.

705

706 Fig. 12 Average highest and lowest temperatures observed for the minimum and maximum $\text{pH}_{\text{insitu}}$ data
707 for each prefecture. The blue and red lines and shading indicate the average and one standard
708 deviation from the average, respectively. The prefectures that met the threshold of 17 are shown in
709 purple, as in Figs. 9 (c–l) and 11 (c–l).

710

711 Fig. 13 Same as Fig. 7, but showing the highest and lowest temperature trends at 289 sites (selected
712 by quality control step 3).

713

714 Fig. 14 Correlation between trends in total nitrogen (TN) and trends in (a) minimum and (b) maximum
715 $\text{pH}_{\text{insitu}}$. The correlation coefficients are -0.30 and -0.29 for the minimum and maximum $\text{pH}_{\text{insitu}}$,
716 respectively (significance level of 0.05, $r = 0.128$; degrees of freedom = 236).

717

718 Table 1 Number of samples (N) collected at each of the 1481 monitoring sites each year.

719

720 Table 2 Average mutual correlation coefficients among water temperature and $\text{pH}_{\text{insitu}}$ measurements at
721 adjacent monitoring sites in the same prefecture. The averages were calculated from the data for the
722 highest and lowest temperature, and minimum and maximum $\text{pH}_{\text{insitu}}$ within 15 km for the three
723 criteria. We refined the sites using three quality control steps, yielding 1481 (step 1), 1127 (step 2),
724 and 302 (step 3) sites. The two columns on the right show the significance level of 5% and the degrees
725 of freedom for the correlation coefficients of each quality check procedure.

726

727 Table 3 Average correlation coefficients between minimum and maximum $\text{pH}_{\text{insitu}}$ trends and total
728 inorganic nitrogen (TN) ones, respectively. We evaluated this for the data after each quality check

729 procedure. Degrees of freedom in step 1 and 2 are same values, because TN data are not necessarily
730 measured at the whole of pH_{insitu} monitoring sites. The sampling number of monitoring sites at step 1
731 and 2 were therefore the same number. Significant levels of 5% and degrees of freedom are also
732 represented.

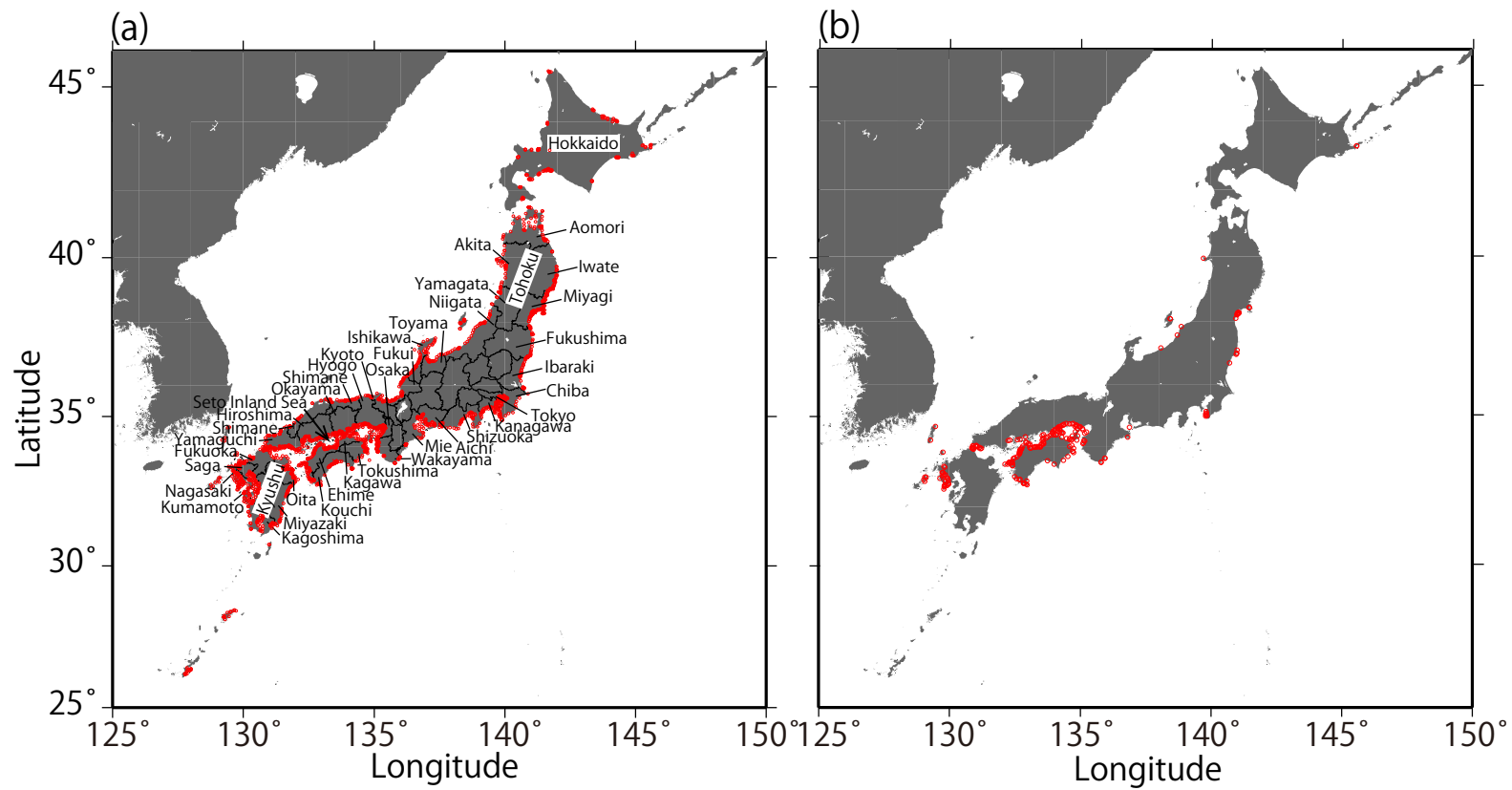


Fig. 1 Coastal maps and monitoring sites in Japan. Red points in (a) indicate the fixed sites ($n = 1481$) monitored by the Regional Development Bureau of the Ministry of Land, Infrastructure, Transport, and Tourism, and the Ministry of the Environment (Japan) under the WCPL monitoring program. (b) Monitoring sites that met the strictest criterion ($n = 302$).

(a) For maximum temperature

(b) For minimum temperature

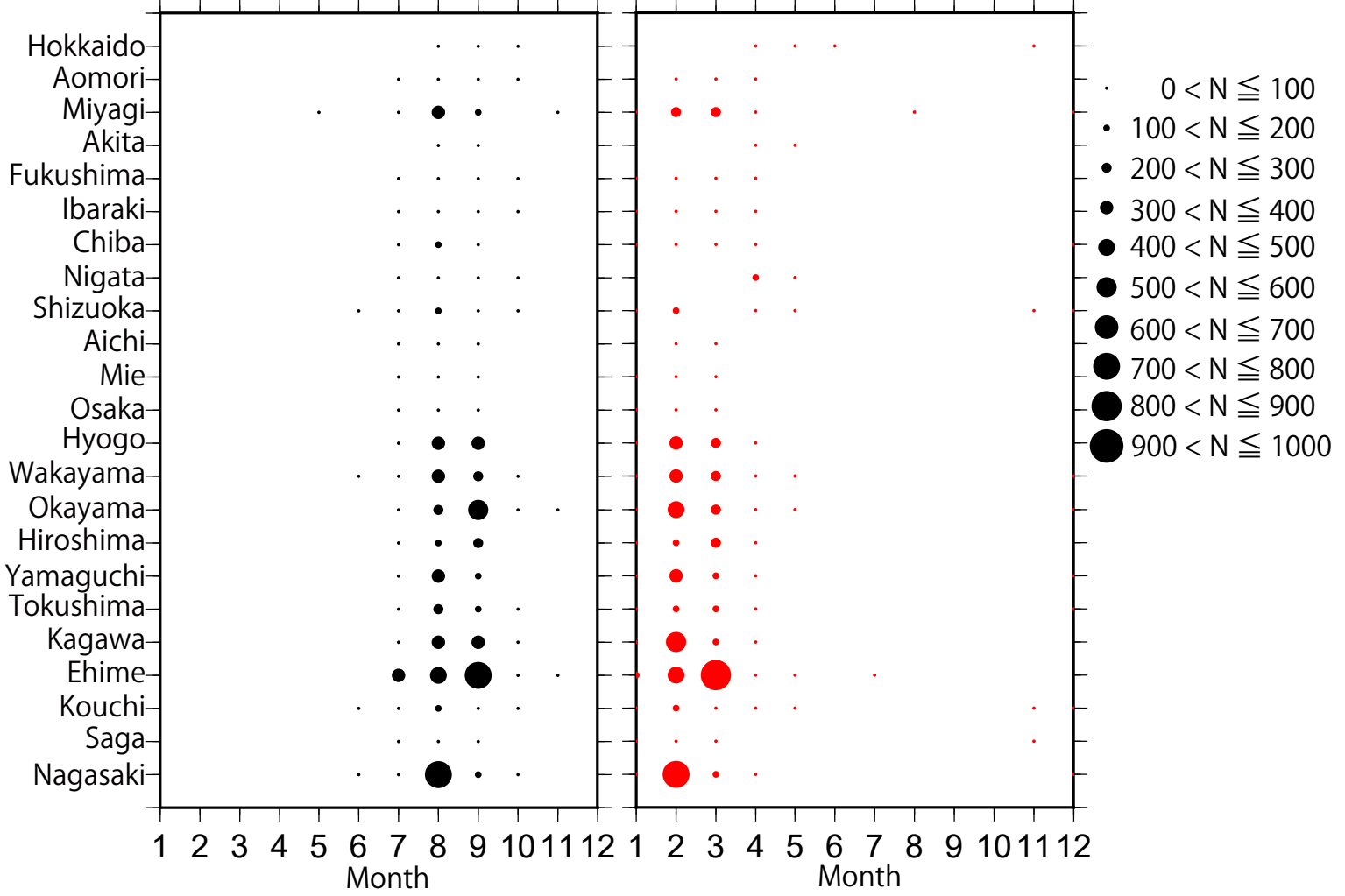


Fig. 2 Distributions of the monthly number of data points (N) for (a) maximum and (b) minimum temperatures collected in each prefecture from the 302 most reliable monitoring sites.

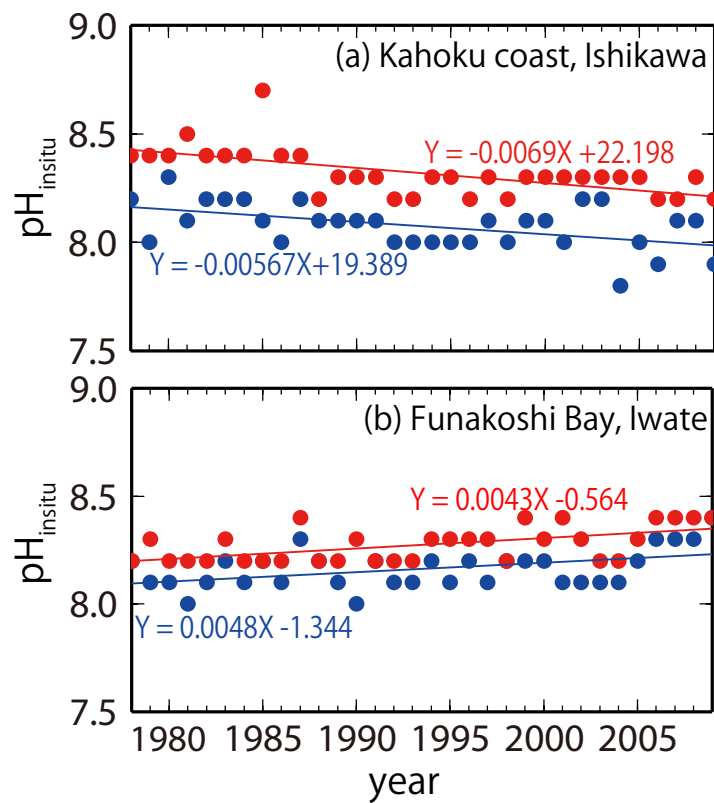


Fig. 3 Examples of (a) acidification (Kahoku Coast in Ishikawa) and (b) basification (Funakoshi Bay in Iwate) trends at monitoring sites. Blue and red colors indicate the annual minimum and maximum pH_{insitu} data and their trends, respectively.

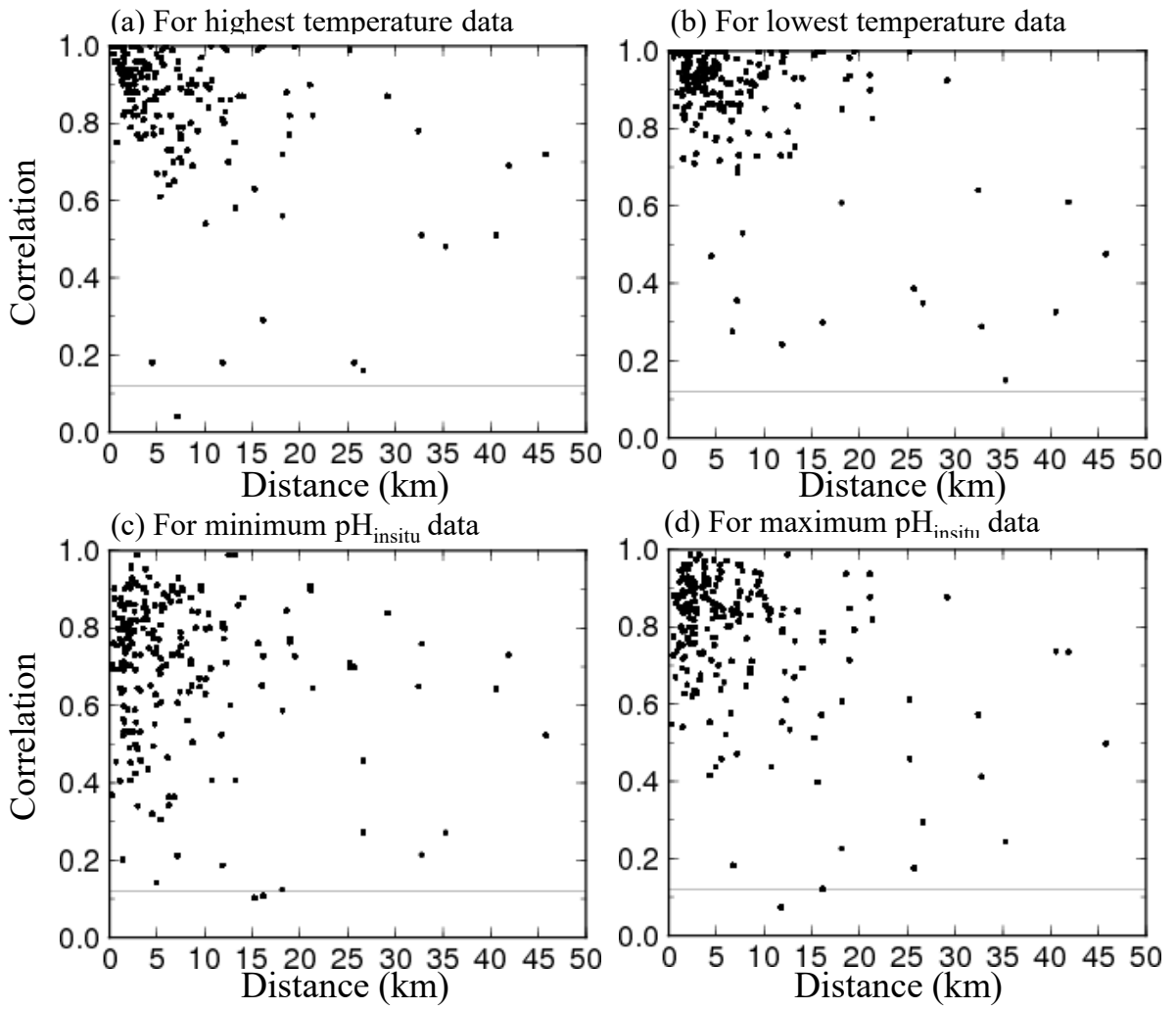


Fig. 4 Correlations of water temperature and $\text{pH}_{\text{in situ}}$ at adjacent monitoring sites in the same prefecture. Thin lines denote significant correlations ($r = 0.12$, degrees of freedom = 283).

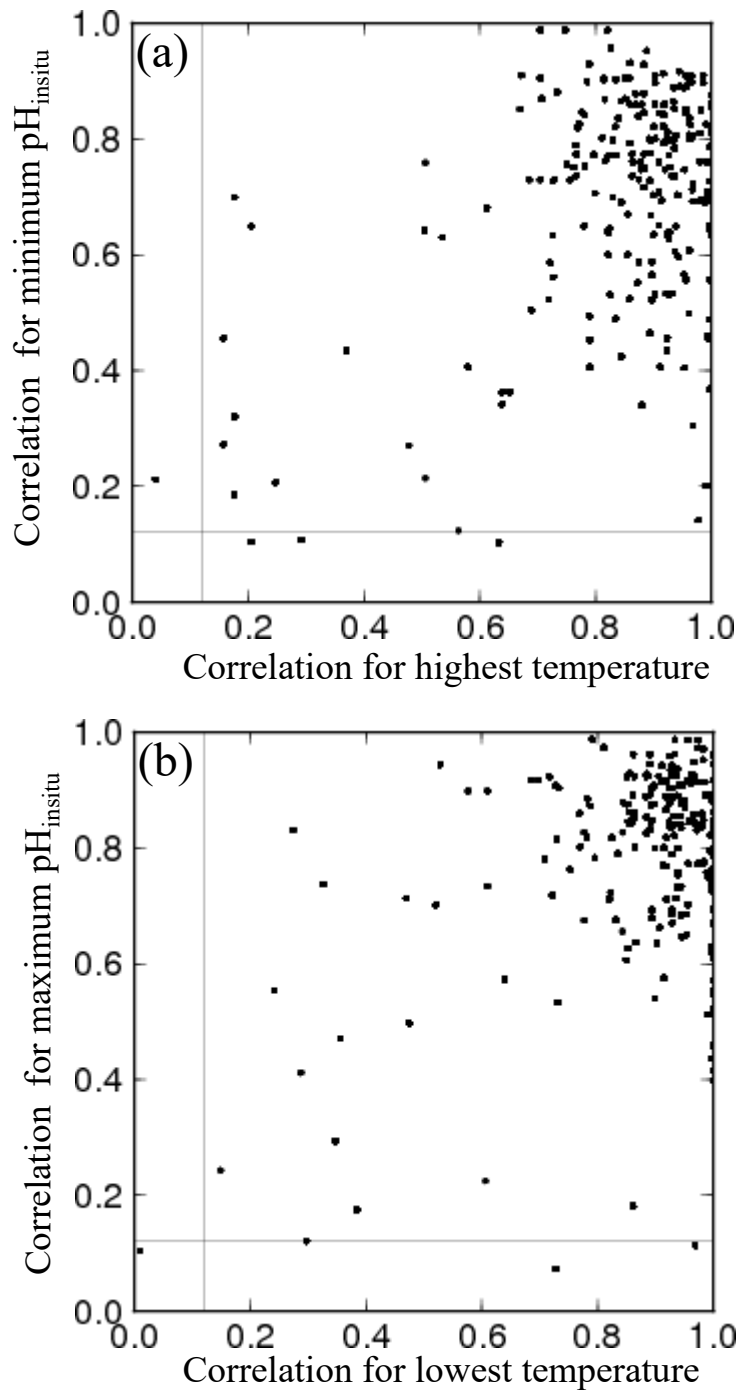


Fig. 5 Scatter plots of correlation coefficients for water temperature and $\text{pH}_{\text{in situ}}$ at adjacent monitoring sites in the same prefecture. Fig. 5a is for the highest temperature and the minimum $\text{pH}_{\text{in situ}}$ data and Fig. 5b for the lowest temperature and the maximum $\text{pH}_{\text{in situ}}$ data, respectively.

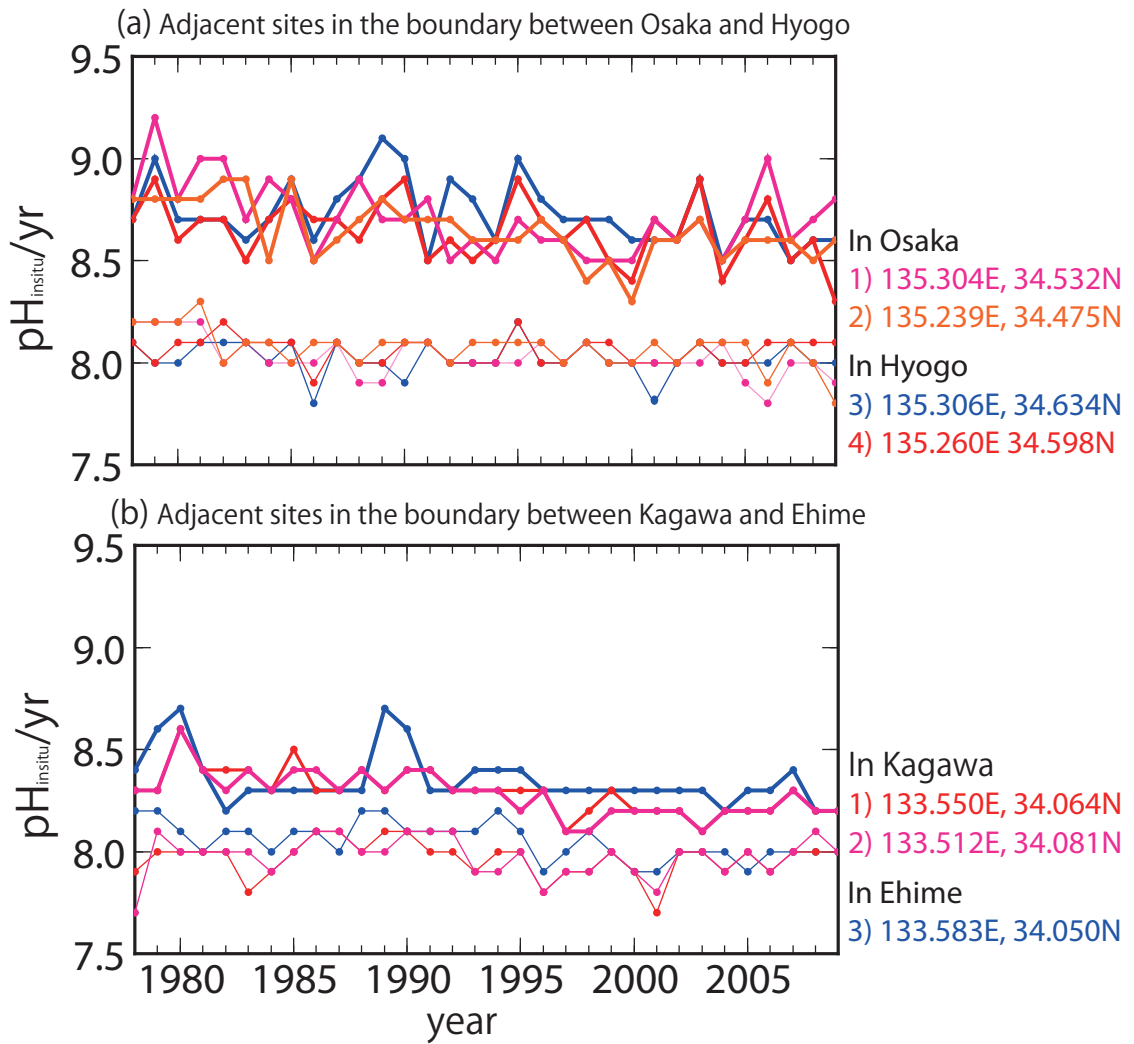


Fig. 6 Examples of time-series for annual minimum and maximum $\text{pH}_{\text{in situ}}$ data at adjacent monitoring sites close to the boundaries between (a) Osaka and Hyogo and (b) Kagawa and Ehime. Lines of the same color indicate data collected at the same site. Thin and bold lines indicate the annual minimum and maximum $\text{pH}_{\text{in situ}}$ data, respectively, at each monitoring stations. Site locations are included to the right of each panel, with the text color corresponding to the colors in each panel.

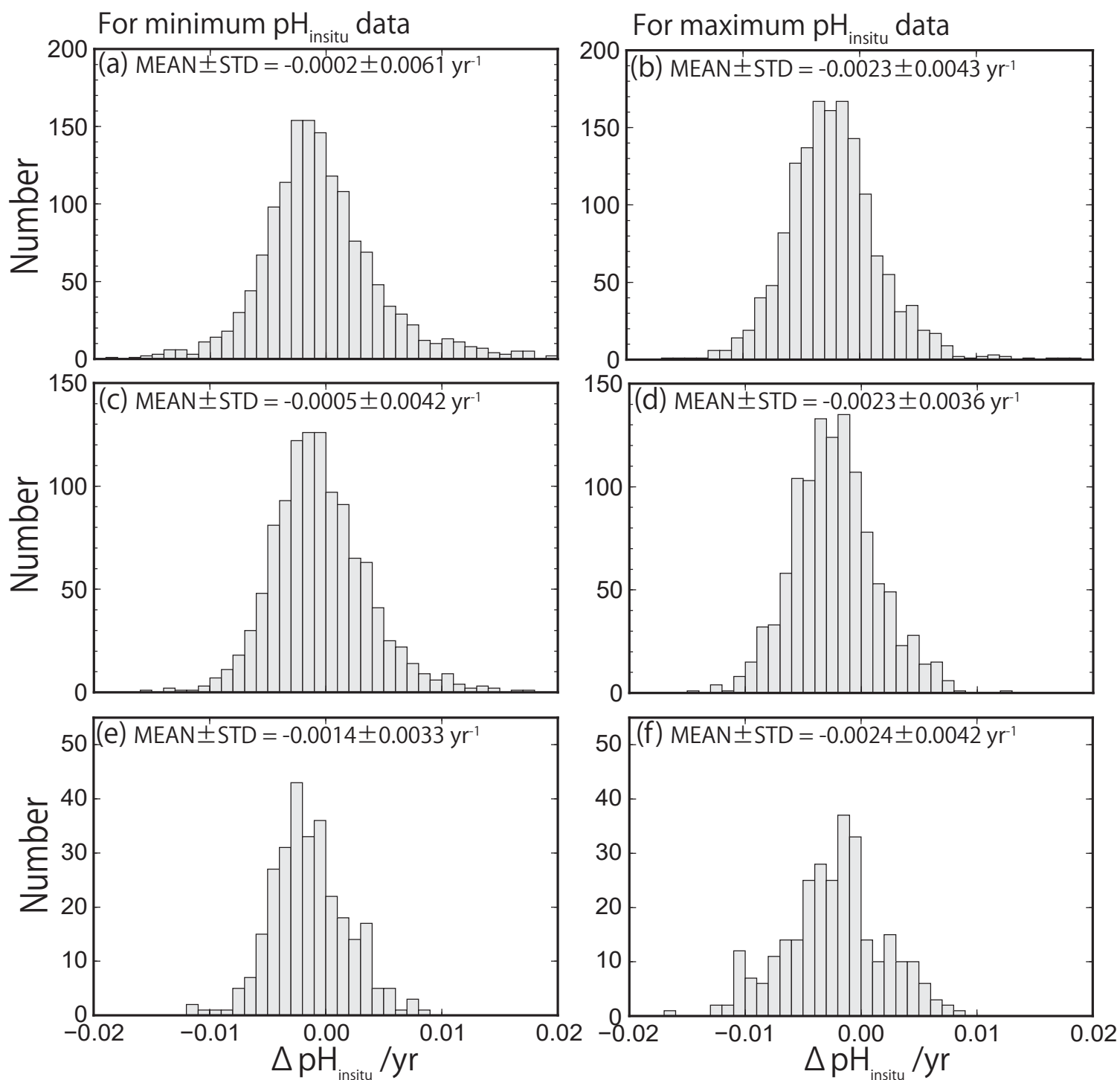


Fig. 7 Histogram of pH trends, represented by $\Delta \text{pH}_{\text{insitu}}$, showing the slopes of the linear regression lines for the annual minimum (left) and maximum (right) $\text{pH}_{\text{insitu}}$ data at each monitoring site. The histograms in (a, b), (c, d), and (e, f) show three scenarios: (a, b) all 1481 available sites with continuous records before quality control, (c, d) 1127 sites without outliers, and (e, f) 289 sites that meet the strictest criterion.

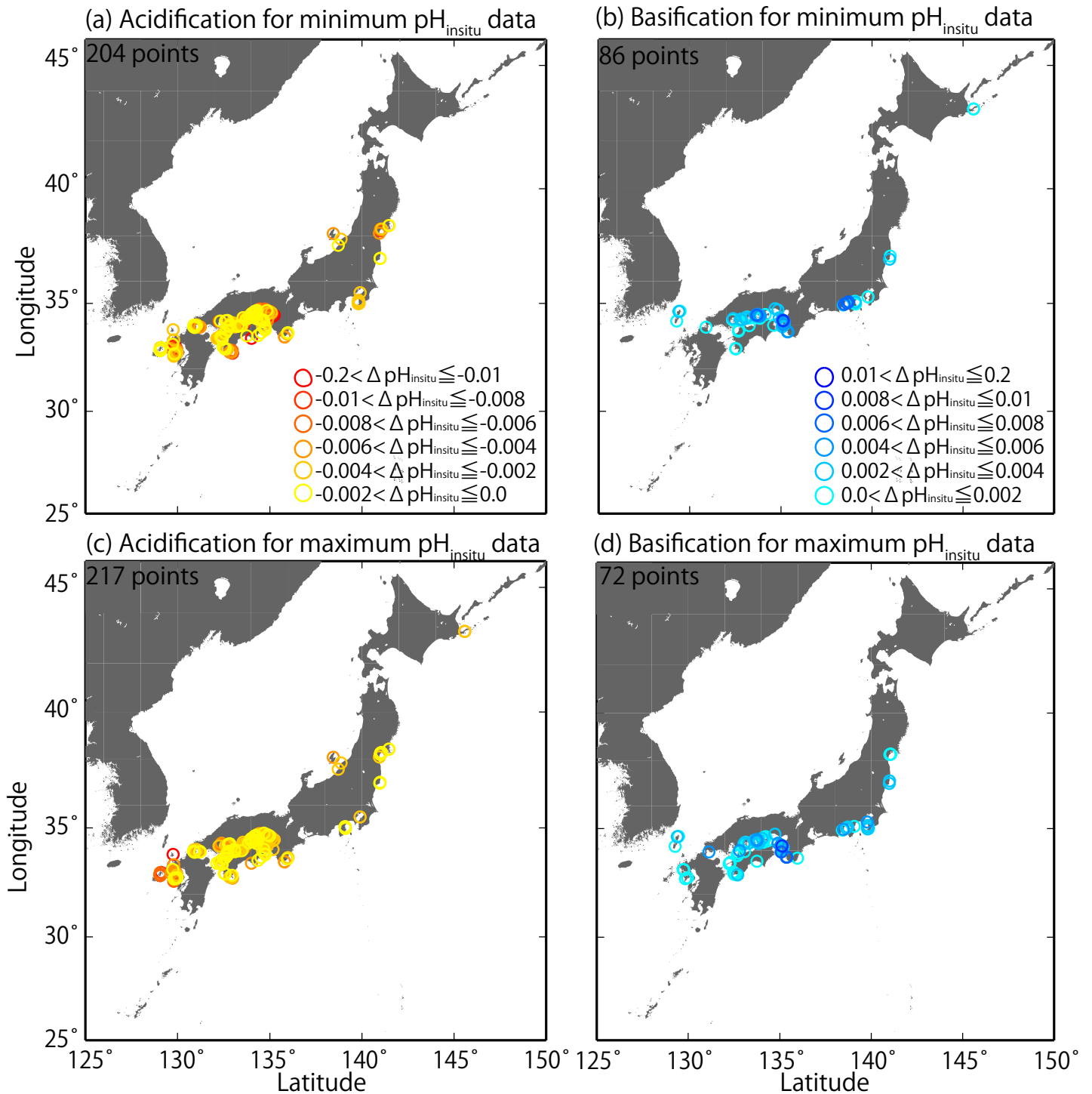


Fig. 8 Distributions of long-term trends in $\text{pH}_{\text{insitu}}$ ($\Delta \text{pH}_{\text{insitu}}/\text{yr}$) in Japanese coastal sea waters. The colors indicate the ranges of acidification (a, c) and basification (b, d). (a, b) and (c, d) are linked to the data used in Figs. 7e and 7f, respectively.

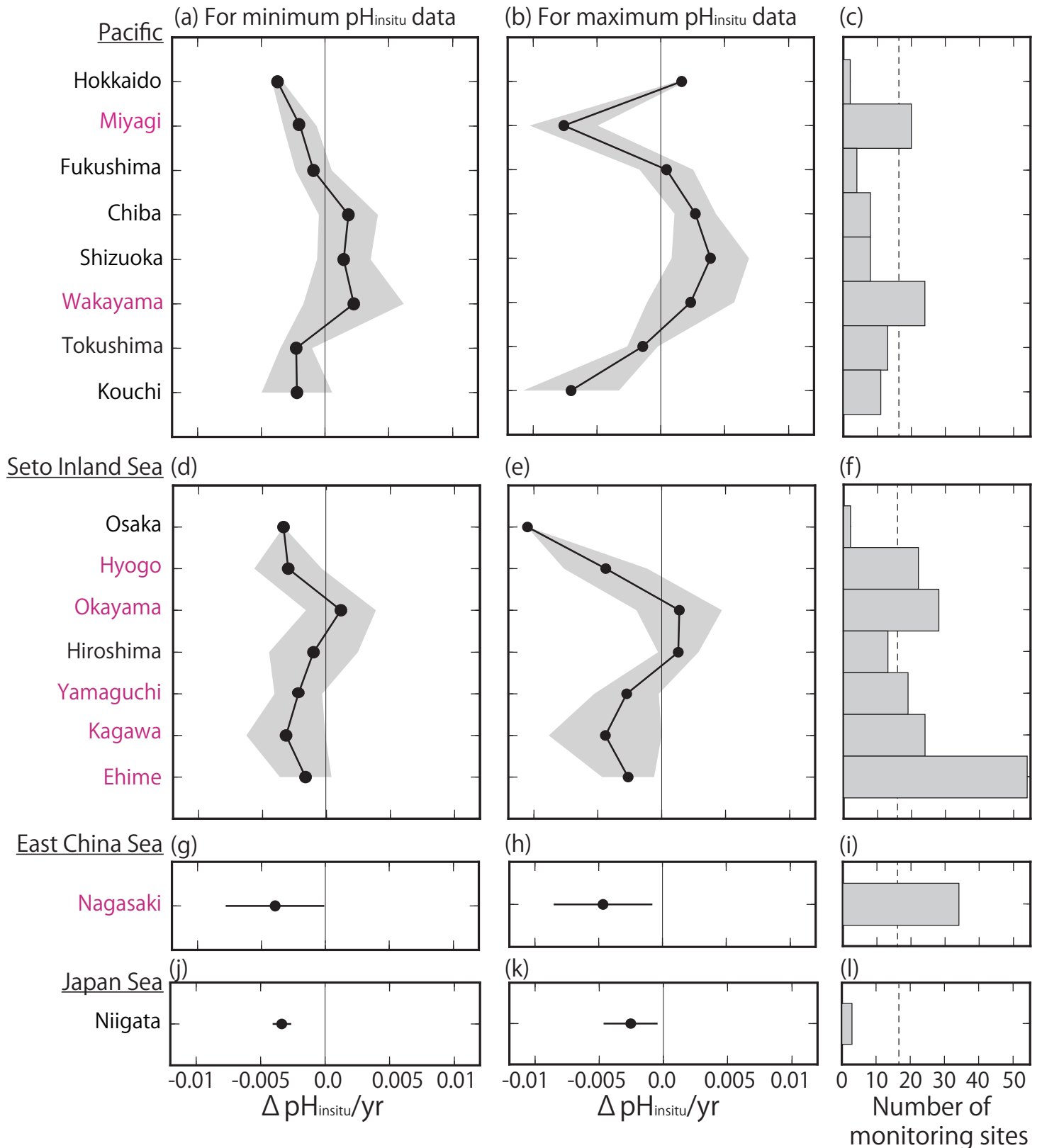


Fig. 9 (a–b, d–e, g–h, j–k) Average minimum and maximum $\text{pH}_{\text{insitu}}$ trends ($\Delta\text{pH}_{\text{insitu}}/\text{yr}$) in each prefecture. These figures show each side of the Pacific (a–b), the Seto Inland Sea (d–e), the East China Sea (g–h), and the Japan Sea (j–k). The prefecture names are arranged vertically from eastern (northern) to western (southern) areas. Black shading indicate one standard deviation from the average. (c, f, i, l) Number of monitoring sites in each prefecture and the thin dashed line is the threshold value of 17 (i.e., the average number of monitoring sites in all prefectures). The prefectures that meet the threshold are indicated in purple. The figure is based on the results shown in Figs. 7 (e, f) and 8.

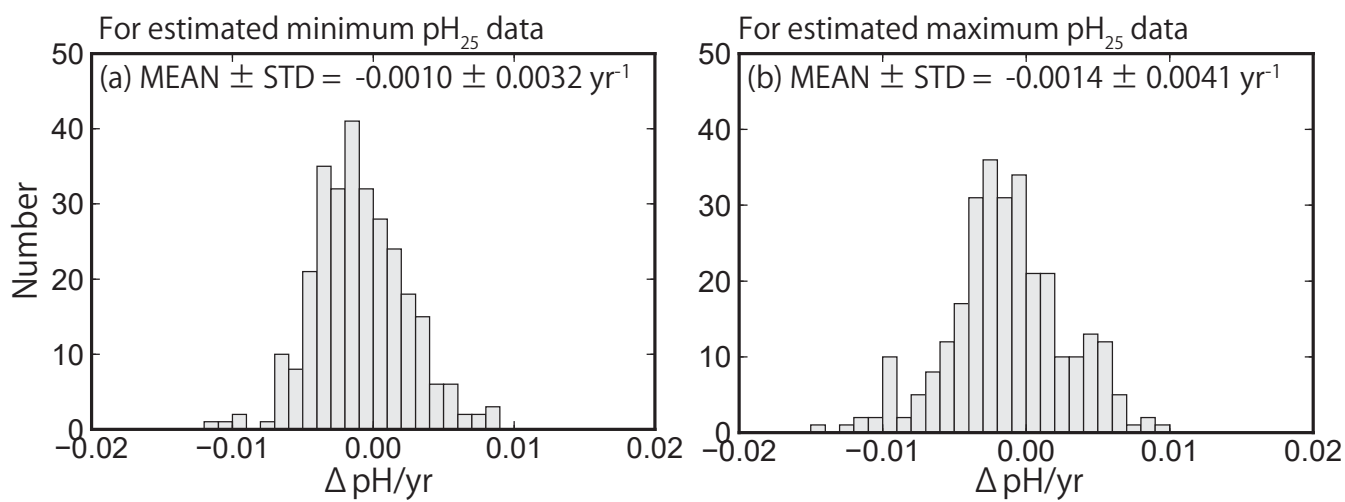


Fig. 10 Same as Fig. 7, but showing the pH_{25} trends at 289 sites (selected by quality control step 3). The value of pH_{25} was estimated using the method of Lui and Chen (2017).

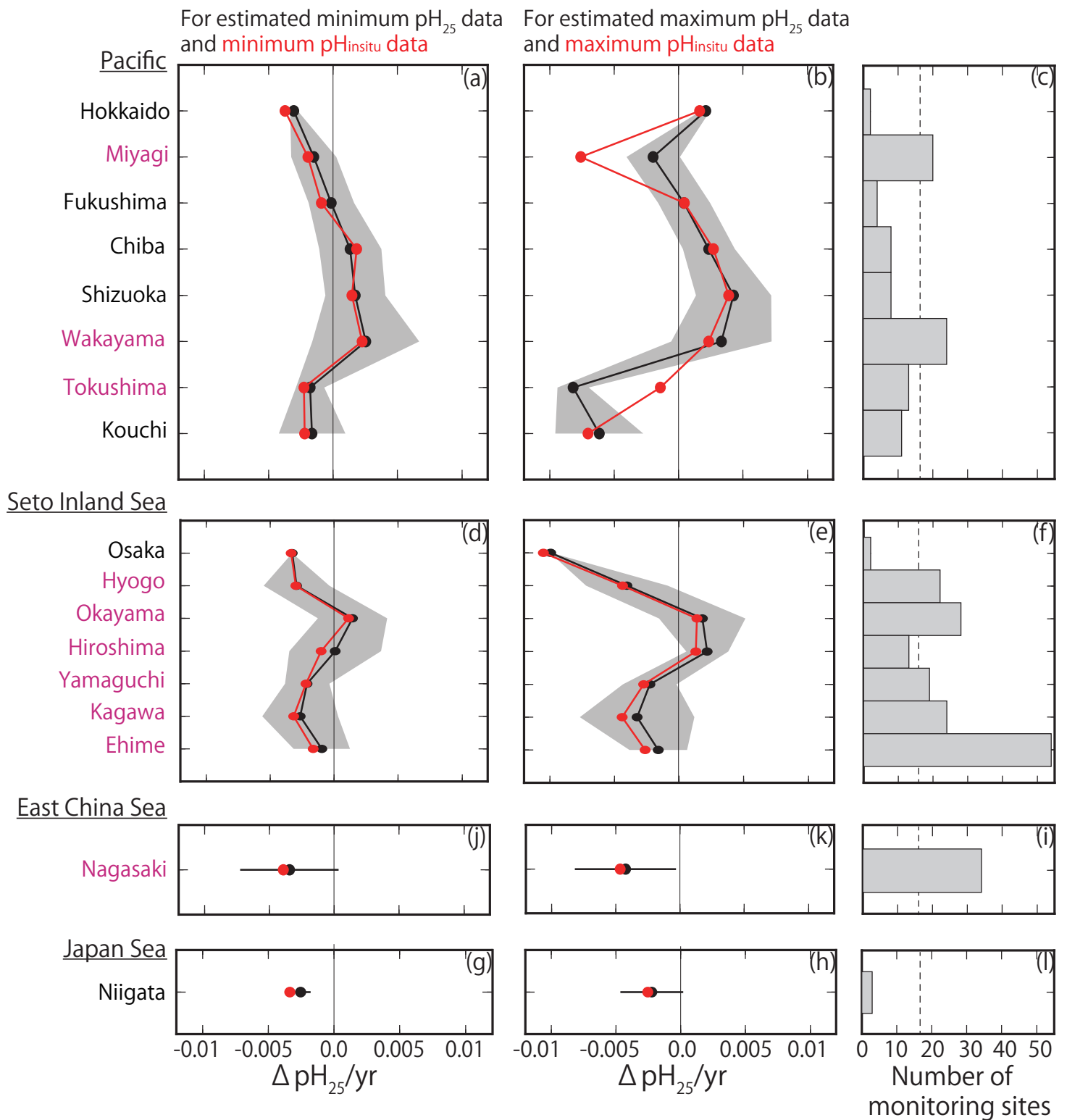


Fig. 11 (a–b, d–e, g–h, j–k) Same as Fig. 9, but showing the average estimated minimum and maximum pH_{25} trends ($\Delta pH_{25}/yr$) for each prefecture. Red lines and points indicate the average minimum and maximum pH_{insitu} trends shown in Fig. 9.

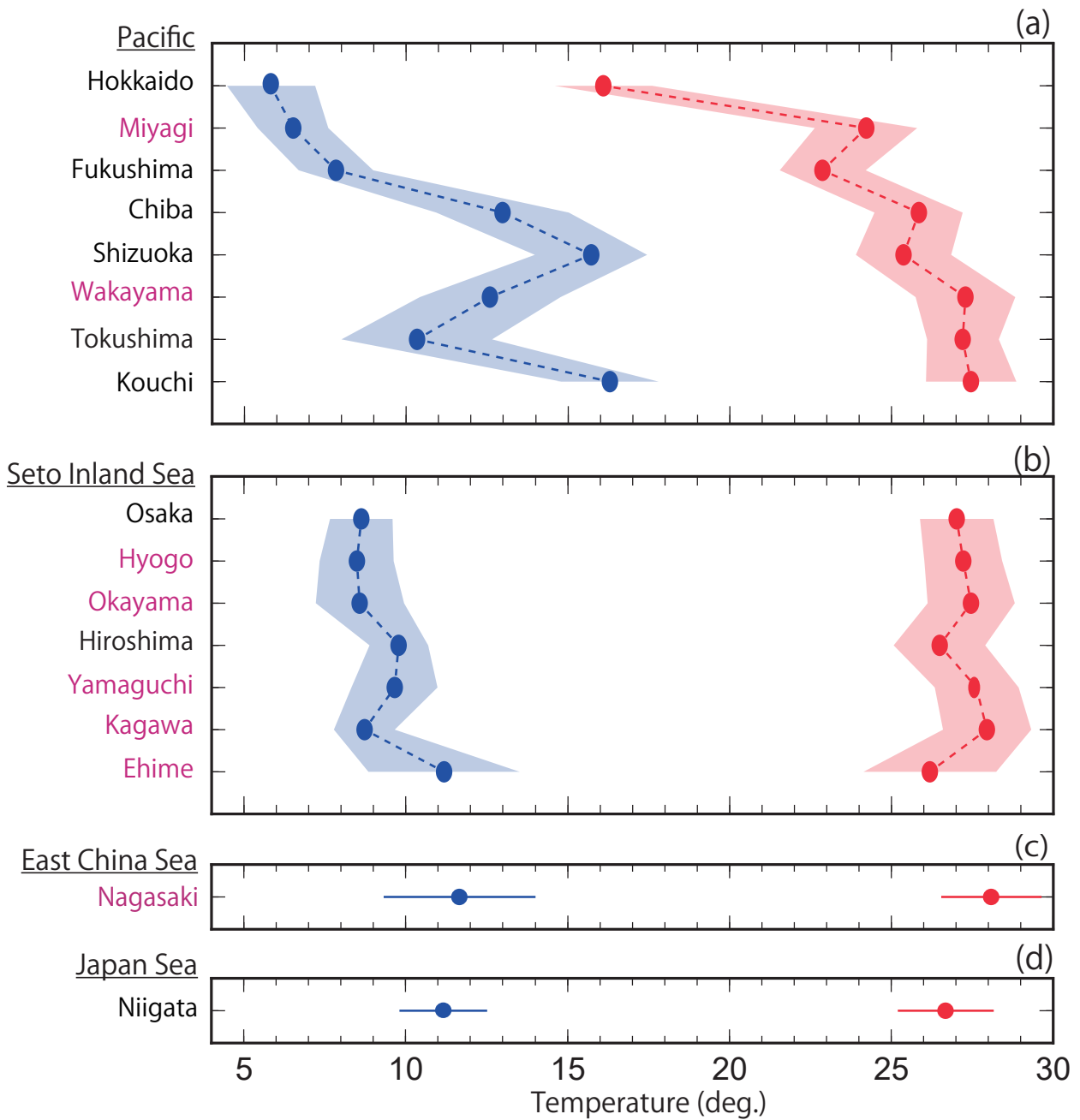


Fig. 12 Average highest and lowest temperatures observed for the minimum and maximum pH_{insitu} data for each prefecture. The blue and red lines and shading indicate the average and one standard deviation from the average, respectively. The prefectures that met the threshold of 17 are shown in purple, as in Figs. 9 (c-l) and 11 (c-l).

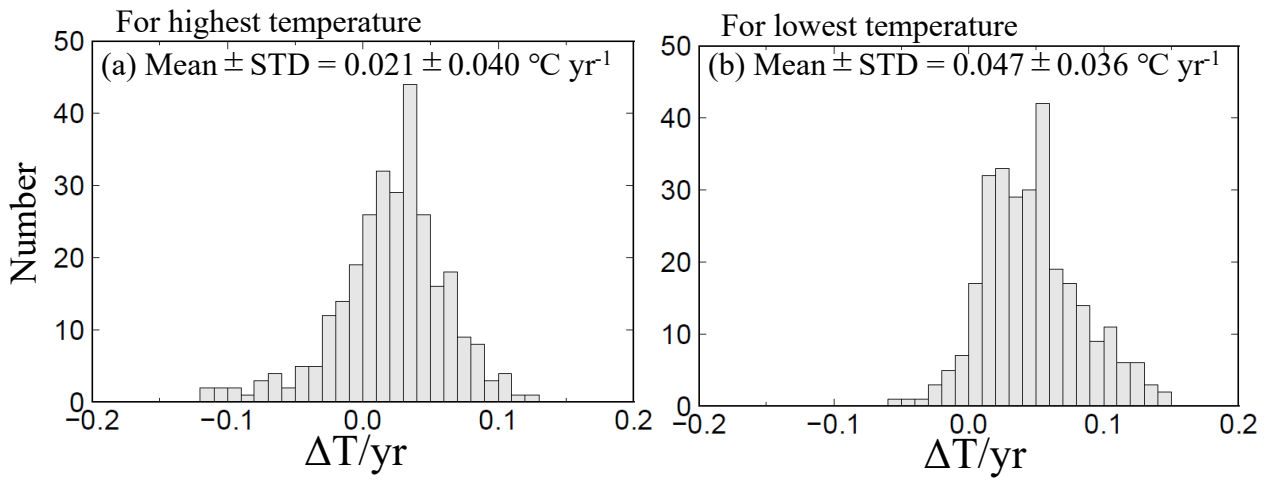


Fig. 13 Same as Fig. 7, but showing the highest and lowest temperature trends at 289 sites (selected by quality control step 3).

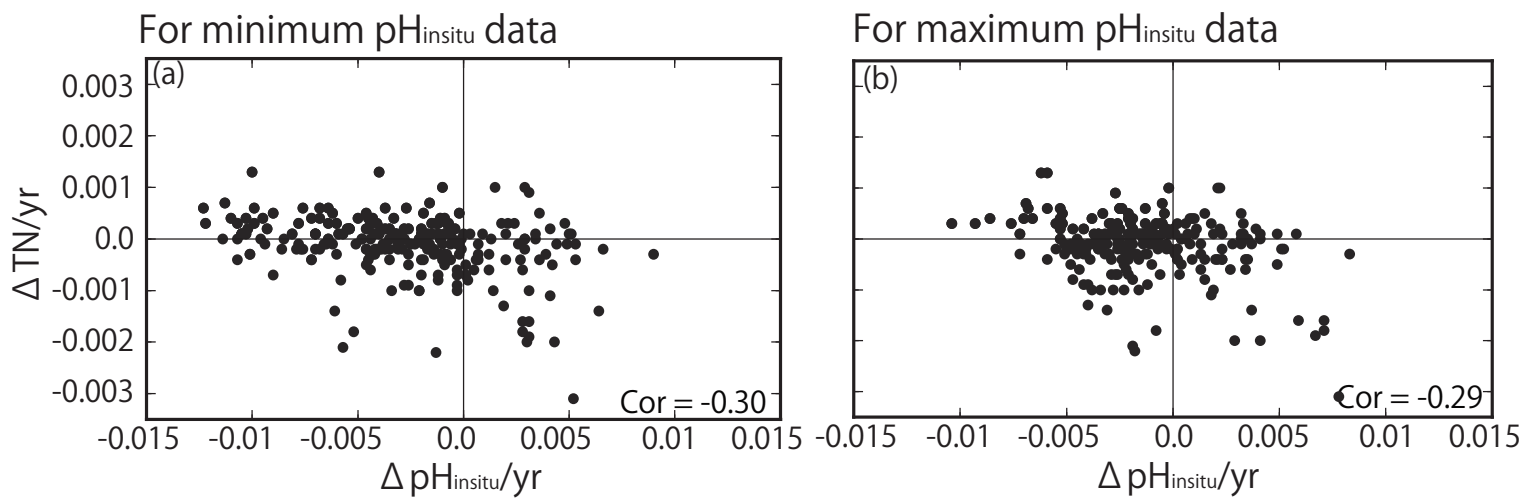


Fig. 14 Correlation between trends in total nitrogen (TN) and trends in (a) minimum and (b) maximum $\text{pH}_{\text{insitu}}$. The correlation coefficients are -0.30 and -0.29 for the minimum and maximum $\text{pH}_{\text{insitu}}$, respectively (significance level of 0.05 , $r = 0.128$; degrees of freedom = 236).

Table 1 Number of samples (N) collected at each of the 1481 monitoring sites each year.

Year	$0 \leq N < 4$	$4 \leq N < 8$	$8 \leq N < 12$	$12 \leq N < 16$	$16 \leq N < 20$	$20 \leq N < 24$	$24 \leq N < 28$	$28 \leq N < 32$	$32 \leq N < 40$
1978	43	391	83	303	87	15	176	9	4
1979	31	372	73	328	101	19	150	11	7
1980	32	363	88	324	101	15	192	12	5
1981	24	347	72	361	99	13	199	11	3
1982	25	350	74	364	93	9	206	11	4
1983	32	355	75	356	91	11	222	12	0
1984	28	362	74	355	96	10	211	11	3
1985	24	354	86	377	96	9	192	11	8
1986	25	361	81	334	98	8	235	11	9
1987	26	357	78	341	98	4	239	11	1
1988	25	366	74	356	82	6	236	11	2
1989	26	365	83	344	84	5	238	17	3
1990	24	377	76	347	83	1	238	14	5
1991	24	367	80	355	93	5	226	13	5
1992	24	367	79	352	95	1	230	16	0
1993	17	374	76	357	94	8	225	14	0
1994	17	376	85	347	102	24	208	14	3
1995	29	376	109	311	104	3	227	12	0
1996	19	419	80	307	104	4	226	14	1
1997	20	396	82	315	115	5	225	13	0
1998	16	389	103	325	99	0	225	12	0
1999	17	396	68	381	67	2	224	12	7
2000	17	389	82	376	72	1	231	6	2
2001	17	392	90	382	50	8	220	6	1
2002	17	368	102	392	49	1	229	7	0
2003	17	365	93	402	51	1	233	6	1
2004	17	370	84	400	50	1	240	5	2
2005	16	354	152	356	46	9	228	3	0
2006	16	370	134	345	50	0	244	5	3
2007	17	399	128	353	62	0	202	5	3
2008	17	402	128	350	64	0	211	5	1
2009	17	403	143	340	58	0	217	5	8

Table 2 Average mutual correlation coefficients among water temperature and $\text{pH}_{\text{insitu}}$ measurements at adjacent monitoring sites in the same prefecture. The averages were calculated from the data for the highest and lowest temperature, and minimum and maximum $\text{pH}_{\text{insitu}}$ within 15 km for the three criteria. We refined the sites using three quality control steps, yielding 1481 (step 1), 1127 (step 2), and 302 (step 3) sites. Two right columns represent a significant level of 5% and a degree of freedom for the correlation coefficients of each quality check procedure.

Quality check procedue	highest temperature data	lowest temperature data	minimum $\text{pH}_{\text{insitu}}$ data	maximum $\text{pH}_{\text{insitu}}$ data	Significance level of 5%	Degree of freedom
1	0.79	0.78	0.51	0.64	0.10	386
2	0.80	0.79	0.54	0.69	0.15	170
3	0.85	0.87	0.62	0.72	0.25	59

Table 3 Average correlation coefficients between minimum and maximum $\text{pH}_{\text{in situ}}$ trends and total inorganic nitrogen (TN) ones, respectively. We evaluated this for the data after each quality check procedure. Degrees of freedom in step 1 and 2 are same values, because TN data are not necessarily measured at the whole of $\text{pH}_{\text{in situ}}$ monitoring sites. The sampling number of monitoring sites at step 1 and 2 were therefore the same number. Significant levels of 5% and degrees of freedom are also represented.

Quality check procedue	Correlation between minimum $\Delta \text{pH}_{\text{in situ}}$ and ΔTN	Correlation between maximum $\Delta \text{pH}_{\text{in situ}}$ and ΔTN	Significant level of 5%	Degree of freedom
1	-0.02	-0.29	0.08	622
2	-0.02	-0.29	0.08	622
3	-0.33	-0.35	0.14	215